AD

TECHNICAL REPORT ECOM-2602

STUDY OF AN M-TYPE BACKWARD-WAVE OSCILLATOR UTILIZING AXIAL BEAM INJECTION

BY

GUNTHER E. WURTHMANN

PARK RICHMOND

PAUL FISCHER

JUNE 1965

ECOM
UNITED STATES ARMY ELECTRONICS COMMAND · FORT MONMOUTH, N.J.

DDC AVAILABILITY NOTICE

Qualified requesters may obtain copies of this report from Defense Documentation Center, Cameron Station, Alexandria, Virginia 22314.

This report has been released to the Clearinghouse for Federal Scientific and Technical Information, U. S. Department of Commerce, Springfield, Virginia 22151, for sale to the general public.

Disclaimer

The citation of trade names and names of manufacturers in this report is not to be construed as official Government indorsement or approval of commercial products or services referenced herein.

Disclaimer

The findings in this report are not to be construed as an official Department of the Army position, unless so designated by other authorized documents.

Disposition

Destroy this report when it is no longer needed. Do not return it to the originator.

Address Change

In case of a change in address, the recipient of this report should notify U. S. Army Electronics Command, Attn: AMSEL–IO–T, Fort Monmouth, N. J.

BLANK PAGE

TECHNICAL REPORT ECOM-2602

STUDY OF AN M-TYPE BACKWARD-WAVE OSCILLATOR UTILIZING AXIAL BEAM INJECTION

By

Gunther E. Wurthmann, Park Richmond, Paul Fischer

Electron Tubes Division
Electronic Components Department

JUNE 1965

DA Task Nr. 1P6-22001-A-055-04-17

U. S. ARMY ELECTRONICS COMMAND
FORT MONMOUTH, N. J.

Abstract

This report reviews the design, fabrication, and testing of a pulsed, re-entrant, M-type backward-wave oscillator (BWO). The tube utilizes a crossed-field gun which feeds the beam axially into the intereaction region, and thus offers a degree of isolation between the gun and the wave structure. The periodic circuit used in this device is an interdigital delay line. Coupling to the external waveguide is accomplished by the use of tapered sections at both ends of the periodic structure.

CONTENTS

FIGURES

BLANK PAGE

STUDY OF AN M-TYPE BACKWARD-WAVE OSCILLATOR UTILIZING AXIAL BEAM INJECTION

INTRODUCTION

The purpose of this internal program was to conduct an investigation on the feasibility of designing and constructing a pulsed, crossed-field, backward-wave oscillator (BWO) that would utilize axial beam injection. This report will review and discuss the design procedure, the fabrication of the experimental tube, and the test results achieved.

DISCUSSION

The original specifications for the BWO included a power output of 150 kw at a 0.001 duty cycle. The device was to operate over a frequency range of 8500 to 10,500 Mc at an efficiency equal to or higher than 20%. A crossed-field tube having a circular geometry was chosen for this study in order to meet the above requirements. A reentrant structure was chosen for the design because it is more easily fabricated and it makes more efficient use of the electron stream. However, a disadvantage of this system is that the bunched, reentrant beam may create undesired oscillations. The risk of oscillations is decreased by the use of a drift space near the output of the RF circuit. In addition, electrons emitted in the attenuating region will tend to smear the bunching pattern.

The structure was designed to use axial beam injection similar to that used in the General Electric voltage-tunable magnetron, except that this device would operate at higher d-c voltages and at a higher current. Here, the impedance of the accelerator is relatively high, thus it draws only a small current. Axial beam injection was chosen since a lower power driver could operate the device. It is also possible to obtain more current from such a tube than in sole-emitting devices since its axial dimension is not limited to a quarter-wave length. Frequency varies as a function of sole-to-line voltage, whereas power output is relatively insensitive to changes in this voltage.

In sole-emitting tubes, the pole pieces required for producing the appropriate magnetic field are often an integral part of the device. However, in this device, an external electromagnet was used to provide the necessary field to the tube. Thus, no magnetic parts were incorporated internally since this would only tend to distort the field. An advantage to this arrangement is there is less danger in handling the tube near high magnetic fields.

Slow-Wave Structure

Circuit Design

The proper choice of design for the slow-wave structure and the care taken in the fabrication of the designed circuit are critical factors in

determining how successfully a tube will operate. An interdigital delay line was chosen for this device because of the relative ease of construction and its desirable bandwidth, impedance, and thermal characteristics. The interdigital structure was originally designed to operate from 10.5 kMc to as low a frequency as possible. The upper cut-off frequency, designated f_{hco}, was set to a value greater than f_h, the upper end of the operating frequency range of the device. The lower cut-off frequency, f_{lco}, was set as close to zero as possible. In order to achieve this, it was planned to replace the supporting metallic back wall with a ceramic back wall. The lengths of the fingers of the line were set at less than $\lambda min/4$, where λmin is the shortest wave length in the intended tuning range of the M-type BWO.

Dissipation Considerations

In order to determine the other dimensions of the line, the dissipation of the individual fingers was considered. The possible use of one of three materials was explored; these were: copper, molybdendum, and tungsten. Using the equation

$$\Delta T \approx \frac{K_1}{k} , \qquad (1)$$

where ΔT is the rise in temperature,

K_1 is a constant which is proportional to the power bombarding a surface and related to the line dimensions, and

k is the thermal conductivity of the material being considered.

Taking into consideration the melting temperature and vapor pressure of these materials, the following was concluded: For a given applied power to the fingers of a line of the same over-all dimensions, tungsten has the most desirable characteristics and molybdenum the least, with regard to melting and vapor pressure. Although tungsten has favorable thermal and electrical characteristics, it is extremely difficult to machine and thus was not used in this program.

Molybdenum, which is somewhat more ductile than tungsten, would be easier to work. Its machining characteristics can be compared to cast iron. This material was eliminated as a candidate at this time because of its somewhat less favorable dissipation and vapor pressure characteristics, coupled with the fact that its electrical conductivity is approximately one third that of copper. However, if necessary, conductivity could be improved by copper-plating the molybdenum structure.

OFHC copper is difficult to work with due to its excessive ductility. However, this material was chosen because of its other advantageous physical properties, plus the fact that considerable fabrication experience was gained with copper from other work with similar type tubes.

In order to determine the finger dimensions, the following equation was used:

$$\Delta T = \frac{P_d L}{k A} , \qquad (2)$$

where

ΔT is the difference in temperature in degrees C between the melting point of copper and the temperature at the base of the finger, which is water-cooled to below 100°C;

L is the length of the finger in meters;

A is the cross-sectional area of the finger in square meters;

P_d is the power dissipation of a finger in watts; and

k is the coefficient of thermal conductivity.

A reasonable estimate is made of the maximum power which might be dissipated on any one finger of the line. In the case of this device, it was approximately 75 watts. Equation (2) is solved for the area, and then by assuming one of the dimensions, the other dimension may be found.

Phase Delay Factors

The delay factor over the band is given by

$$\frac{c}{v} = 2\frac{\lambda}{p} - \frac{L}{p} , \qquad (3)$$

where c is the velocity of light in meters;

v is the phase velocity in meters;

λ is the operating free space wave length in meters,

p is the pitch between adjacent fingers in meters; and

L is the length of delay line finger in meters.

A graph of the delay ratio of the circuit under consideration versus the wave length is shown in Figure 1. As can be noted, the delay ratio increases the wave length; thus, the phase velocity increases with frequency. Under oscillation conditions, the phase velocity is synchronous with the electron velocity. The electron velocity is directly proportional to the electric field between the sole and the delay line, and inversely proportional to the magnetic field. It is expressed by

$$v_e = E/B , \qquad (4)$$

where v_e is the electron velocity in meters:

E is the field between the delay line and sole in volts/meter; and

B is the orthogonal magnetic field in webers/meters^2.

Using the expressions for phase and electron velocity, one obtains the equation relating frequency to the sole-to-line voltage.

$$f = \frac{V_{sl}}{2p\,Bd\,(1+ L/c\ V_{sl}/pBd)} \qquad (5)$$

where

f is the frequency in cycles per second,

V_{sl} is the sole-to-line voltage in volts, and

d is the distance from the sole to the line in meters (other parameters as previously defined).

Figure 2 shows the theoretical curve relating frequency to tuning voltage.

Delay Line Considerations

The sole, an electrode which is used for establishing the proper electrostatic field through which the beam may move, is positioned essentially concentric with the delay line. Because of its position relative to the delay line, it affects the pass band of that structure. Cold-test measurements should be taken with this electrode in place in order to ascertain that no radical shift in the design parameters occurs.

The delay circuit is coupled to the rectangular waveguide by means of a ridge waveguide, which is tapered from the delay line to the output window. The input impedance of the delay line is estimated by using an approximate equation for the parallel strip transmission line, as follows:

$$Z_{in} = \sqrt{\frac{\mu}{\epsilon}}\,\frac{s}{s+h}\ , \qquad (6)$$

where

Z_{in} is the strip-line impedance in ohms,

s is the spacing between fingers in meters,

h is the depth of the fingers in meters,

μ is the permeability of free space, and

ϵ is the permittivity of free space.

A linear section of the proposed delay line was constructed for cold-test purposes. The matching of this line to the rectangular X-band waveguide was accomplished with a tapered section. The line dimensions are as follows:

finger length - - - - - - - - 0.5 cm

finger depth - - - - - - - - 0.25 cm

finger width - - - - - - - - 0.05 cm

spacing between fingers - - 0.05 cm

length of tapered section - 10 cm.

Curves of return loss and insertion loss are shown in Figures 3 and 4.

Electron Gun Design

One characteristic of the gun structure chosen is its apparent separation from the rf section of the tube. In this design, the surface of the cathode is at least partially protected from the effects of back bombardment. In order to evaluate the original gun design prior to assembly of the final tube, electron trajectories were plotted on the particle trajectory tracer in the Electron Tubes Division, USAEL. The electron ballistic equations in cylindrical coordinates are as follows:

$$\frac{d^2r}{dt^2} - r\left(\frac{d\theta}{dt}\right)^2 = -\frac{e}{m}\left(E_r + r B_z \frac{d\theta}{dt}\right), \qquad (7)$$

$$r\frac{d^2\theta}{dt^2} + 2\frac{dr}{dt}\frac{d\theta}{dt} = \frac{e}{m} B_z \frac{dr}{dt}, \qquad (8)$$

$$\frac{d^2z}{dt^2} = -\frac{e}{m} E_z . \qquad (9)$$

These equations were programmed on an analog computer, and the tentative gun design dimensions were scaled up in size so that a cross-sectional design could be fitted on the Poisson cell for trajectory plots. The trajectory tracer system and a close-up view of the Poisson cell, which simulates the tube geometry, are shown in Figures 5 and 6. The programmed flow diagrams are shown in Figures 7 and 8. Figure 7 shows the program used to obtain equipotential plots of the scaled electrodes. These equipotential plots are shown in Figure 9.

Plots of electron gun trajectories with a cylindrical cathode are shown in Figure 10. In an effort to improve the laminarity of the beam, it was decided to tilt the cathode approximately 10 degrees. Trajectories obtained under this condition are shown in Figures 11 through 14. There appears to be a noticeable improvement in the laminarity of the electron stream when utilizing the tilted cathode. Figure 15 is a plot of trajectories obtained when the magnetic field is increased to 2500 gauss. At this value of magnetic field, the electron trajectories follow a path close to the sole electrode.

Tube Construction and Evaluation

Design and operational data selected for this device are shown below.

Frequency Range	8500 - 10,000 Mc
Peak Power Output	150 kw
Duty Cycle	0.002
Maximum Anode Voltage	30,000 volts
Maximum Accelerator Voltage	12,000 volts
Sole Voltage Approximately	-5,000 volts
Peak Anode Current Approx.	20 amps
Magnetic Field Density	2650 gauss
Estimated Efficiency	25%
Minimum Wave Delay Ratio	(c/v) Min = 10.6
Maximum Wave Delay Ratio	(c/v) Max = 13.25
Cathode Area	4 cm^2
Anode Radius	1.5 cm
Distance anode to sole	d = 0.4 cm
Circuit Pitch	p = 0.1 cm
Finger Length	L = 0.5 cm
Finger Width	w = 0.05 cm
Finger Depth	h = 0.25 cm
Spacing Between Fingers	s = 0.05 cm
Number of Active Fingers	N = 50

During the early phases of the program it was planned to use a ceramic back wall in the construction of this device. However, it was discovered later that the ceramic, although available, could not be obtained with the dimensional tolerances desired. Consequently, a metal back wall was incorporated into the design.

Figure 16 shows a cross-sectional view of the gun and interaction region of the tube. In addition to the gun and interaction circuit already described, it can be seen that a water channel is incorporated in the device for cooling purposes. One wall of this channel forms the back wall of the interdigital circuit. The effect on the circuit, in addition to cooling, is to add reactive loading to the delay line, which tends to raise the lower cutoff frequency. Both ends of the interdigital delay line are coupled to the external waveguide circuit by means of tapered sections. This permits the

direct measurement of insertion loss of the tube. Block diagrams showing the set-ups used in measuring return loss and insertion loss are shown in Figures 17 and 18. Recorded results of the measurements over the operating band are shown in Figures 19 and 20. It is important that the alignment of the fingers be accurately maintained. If this is neglected, stop bands will be created in the operating frequency range. The evacuated portion of the tube is separated from the external waveguide by triple-iris windows. A curve showing the transmission through the window is shown in Figure 21. As noted from the curve, the windows have a negligible effect on the over-all characteristics of the tubes.

Interdigital circuits of this type are necessarily complex and difficult to machine to the desired tolerances. Although the line was fabricated by outside shops which specialize in machining structures of this type, the fingers of the periodic structure were out of alignment enough so that predicted theoretical performance was not realizable in practice.

A block diagram of the hot-test set-up is shown in Figure 22, and a picture of the hot-test station is shown in Figure 23. This test station was used to check the rf transmission through this structure over the operating band. A plot of the insertion loss of the tube measured with this equipment is shown in Figure 24. The tube depicted in Figure 25 utilizes two ports to couple the interdigital circuit to the external waveguide; thus, a check on the tube amplifying characteristics was made using the test set-up shown in Figure 22. The CW signal from the generator is passed into the tube where it is amplified. The detected output pulse, as viewed on the oscilloscope, shows a good reproduction of the input voltage pulse. In Figure 26, several detected scope signals are displayed. Since the operating voltages were extremely low, the gain was also quite limited. The reason the desired voltages could not be attained either in processing or during the test was that the accelerator electrode was tilted from its normal position, which was determined by x-ray examination of the tube.

Discussion of Results

The gun design is such that the electric field is strongest at the exit point of the structure and becomes rapidly weaker as it is moved away from the interaction area. Since the emission is strongly dependent on this field, it is apparent that only a small part of the cathode is effective. In addition to this, any possible back bombardment would first affect the area of the gun nearest the interaction region. One possible solution to the unequal emission problem is that in addition to tilting the cathode, as was done in this device, the accelerator be tilted so that it is nearly parallel to the cathode. This would correct the emission problem which now exists. Corrections in the design of a modified gun could be analyzed using a computer system, after which the beam testers could be constructed for practical analysis.

The interdigital delay line uses a metal back wall to support the line. This back wall shunts the periodic circuit with a varying reactance. In the

present tube, coupling to the external circuit is achieved by means of a tapered section to the external waveguide. The cut-off frequency of the waveguide, and thus the circuit, is limited to approximately 6.6 kMc. It has been suggested that ceramic be used to support the line since the circuit bandwidth would then be increased. One change that might be necessary in a new device is that the coupling to the external circuit would be made using a strip line or coaxial line. In addition, another power supply is then needed to isolate the periodic circuit from the body of the tube.

One of the major problems in devices of this type is the proper alignment of the fingers of the periodic line. Discontinuities in the finger spacings cause high reflections from the circuit which give rise to stop bands in the operating frequency range. Improved tube fabrication techniques now available would solve this problem.

CONCLUSIONS

The results of the evaluation indicate that the design approach pursued is feasible, even though the performance characteristics of the tube fall short of the design goals.

Readily available design and fabrication techniques applied in a straightforward engineering manner would result in the development of a tube with improved electron gun characteristics and improved, slow-wave structure features. This, in turn, would lead to vastly improved over-all tube performance. Due to the high priority of other programs, however, there are no plans at the present time to proceed further with this program.

ACKNOWLEDGMENT

The authors wish to express their appreciation to Messrs. B. Smith, C. LoCascio and C. Matthews of the Techniques Branch for the fabrication and processing of the final test model, and to Messrs. W. Maurer, F. Sherburne and A. Lisper of the Microwave Tubes Branch, for their cooperation in setting up the test equipment for this program.

BIBLIOGRAPHY

1. E. Okress, "Crossed-Field Microwave Devices," Vols I and II, Academic Press, Inc. (1961)

2. J. C. Slater, "Microwave Electronics," D. Van Nostrand Company, Inc. (1950)

3. R. G. E. Rutter, "Beam and Wave Electronics In Microwave Tubes," D. Van Nostrand Company, Inc. (1960)

4. G. B. Collins, "Microwave Magnetrons," McGraw-Hill Company, Inc. (1948)

5. W. J. Kleen, "Electronics of Microwave Tubes," Academic Press Inc. (1958)

6. J. C. Walling, "Interdigital and Other Slow Wave Structures," Electronics and Control, Vol. 3, pp 239-259, March 1957

7. R. C. Fletcher, "A Broad-Band Interdigital Circuit for Use In Traveling-Wave Type Amplifiers," Proc. of the I.R.E., Vol 40, pp 951-958 (1952)

8. S. P. Yu and P. N. Hess, "Slow Wave Structures for M-Type Devices," I.R.E. Transactions on Electron Devices, January 1962.

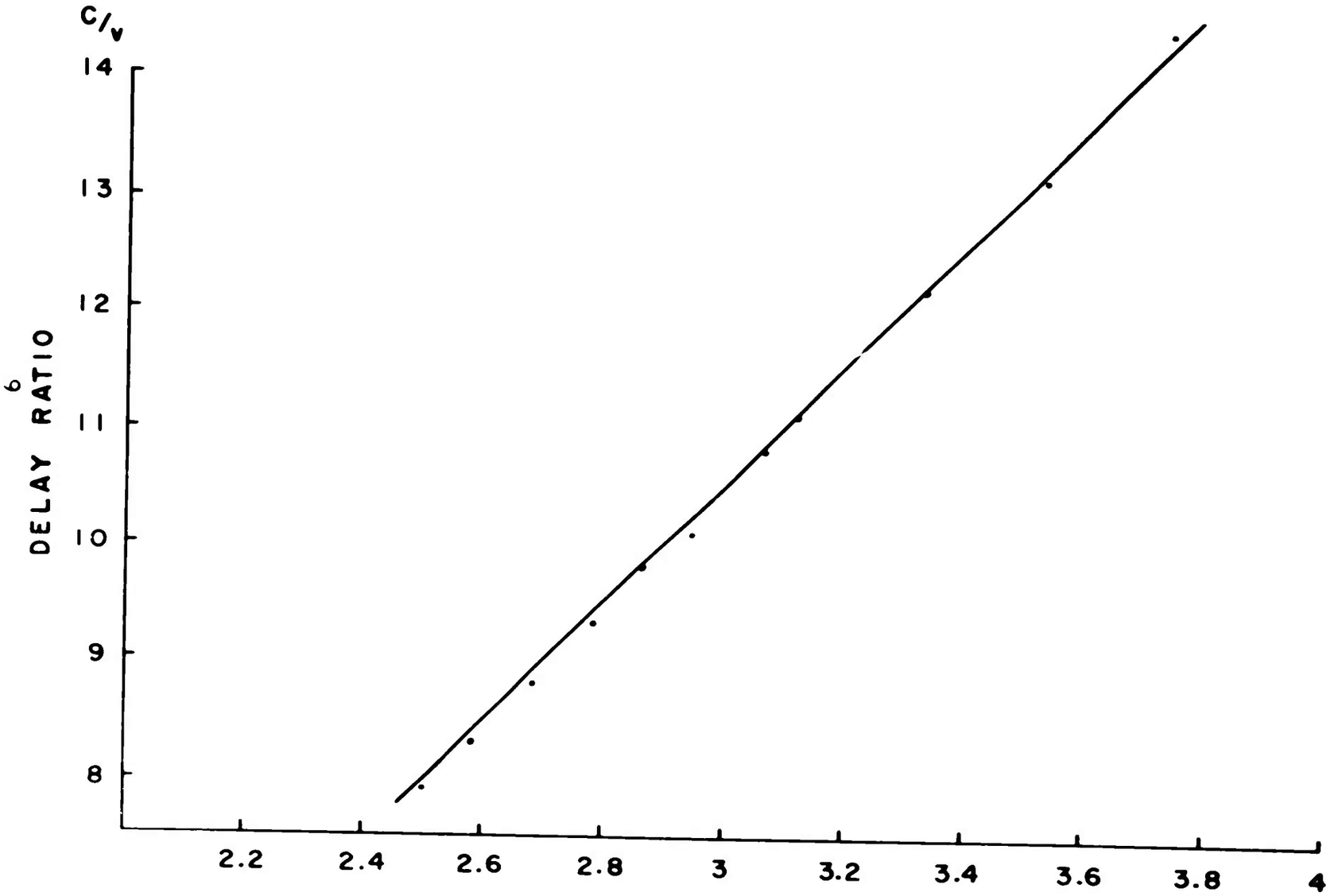

FIG. 1 DISPERSION CURVE

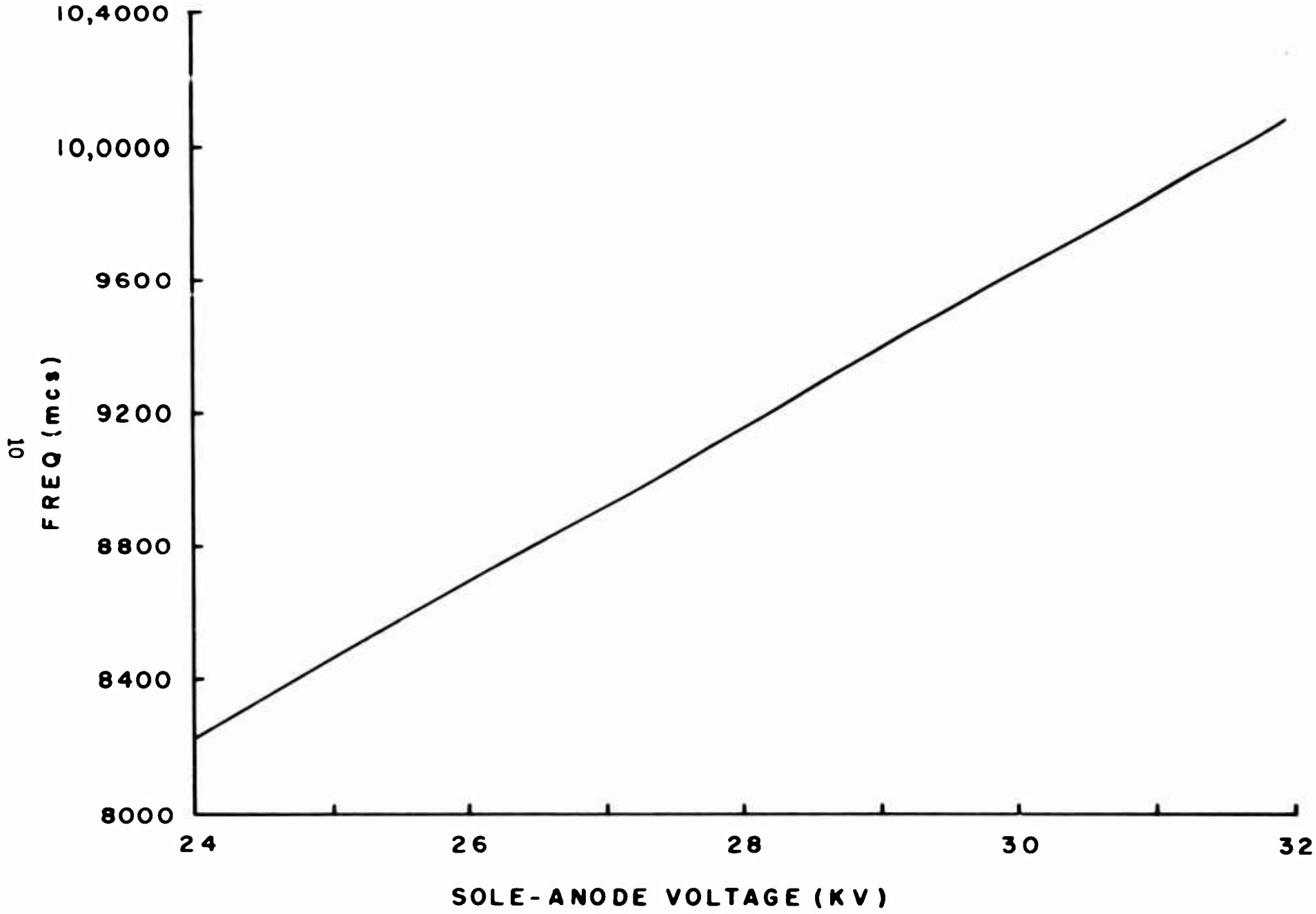

FIG. 2 THEORETICAL TUNING CURVE

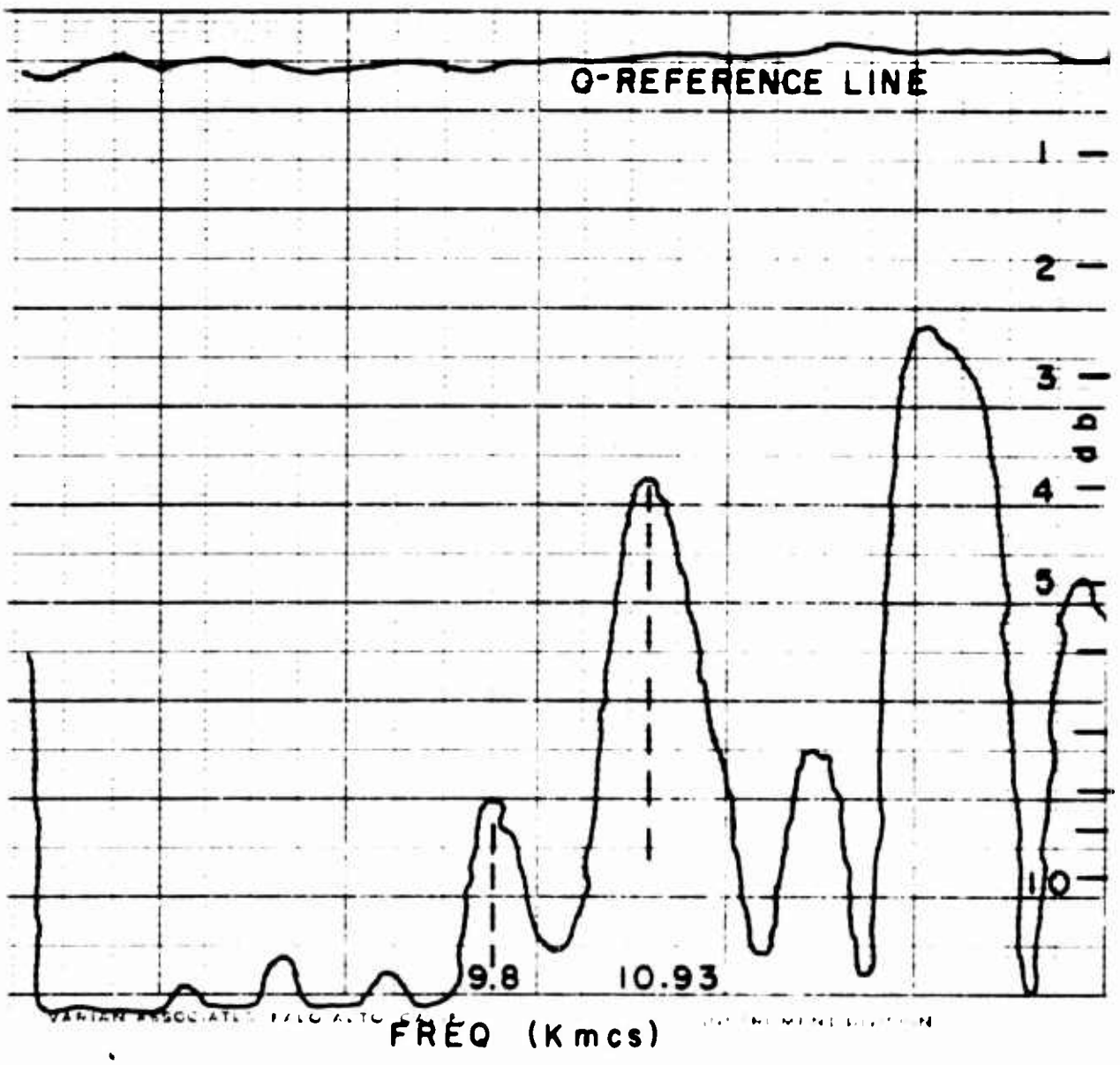

FIG. 3 INTERDIGITAL DELAY LINE
RETURN LOSS IN d b.

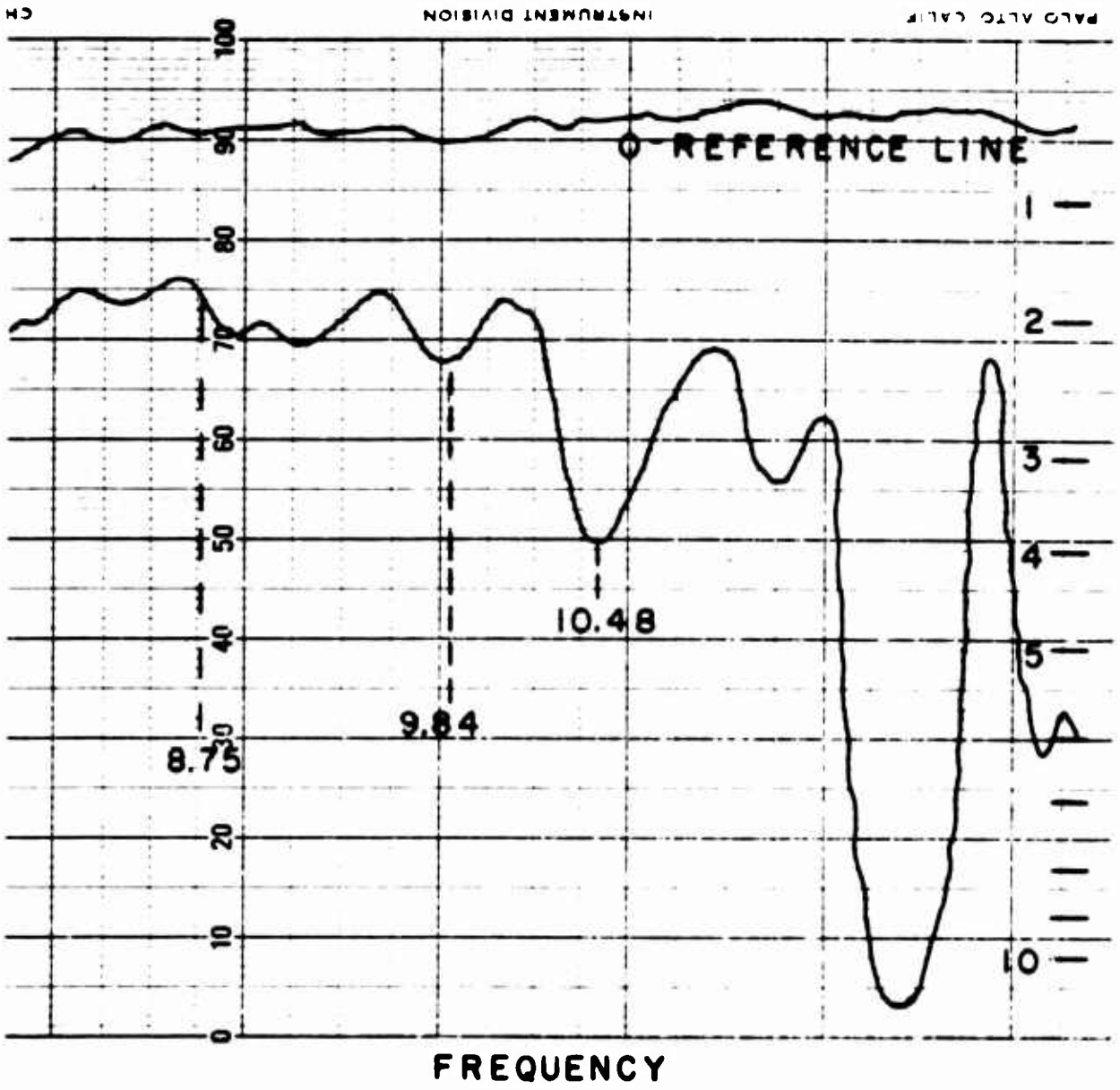

FIG. 4 INTERDIGITAL DELAY LINE INSERTION LOSS CHARACTERISTIC IN db.

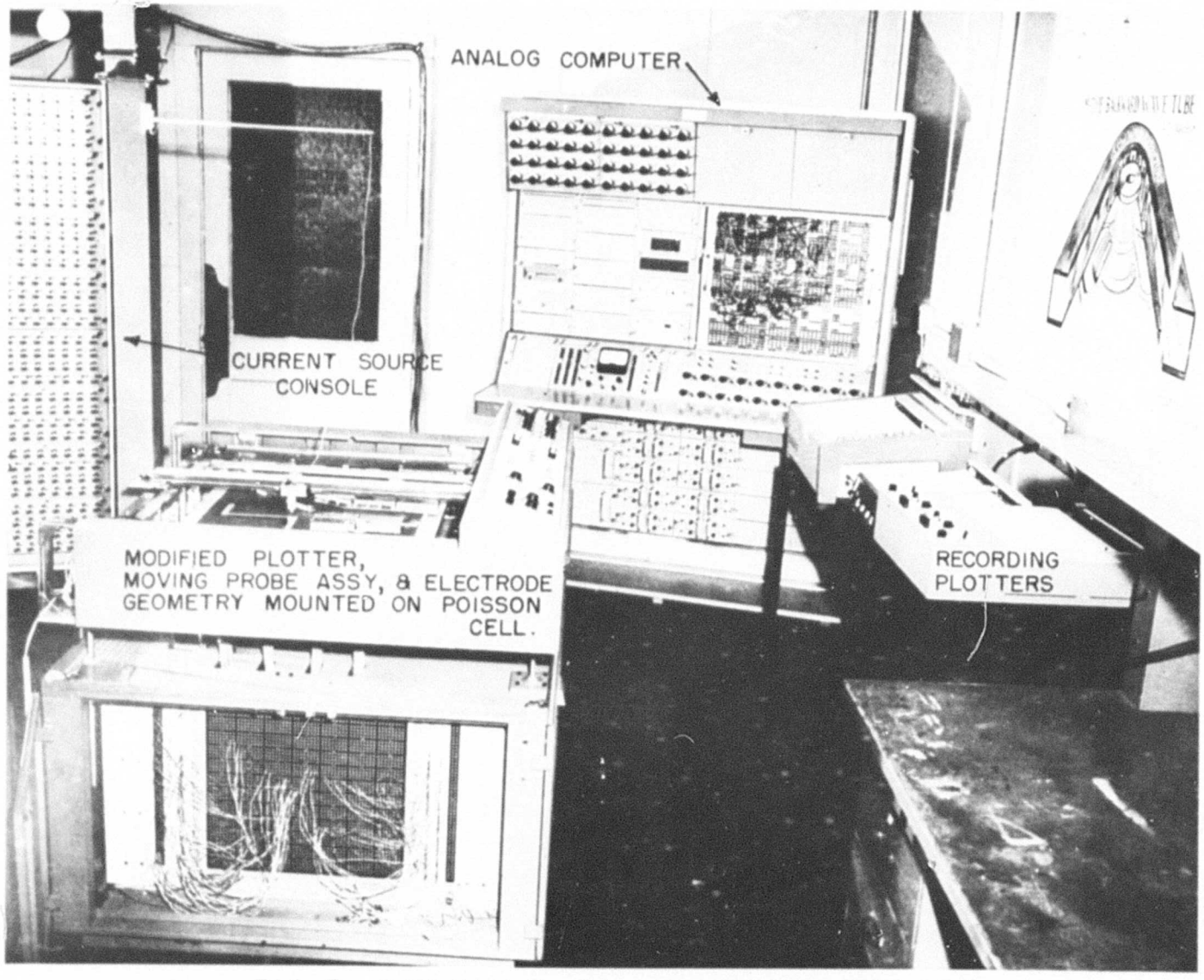

FIG. 5 PARTICLE TRAJECTORY TRACER

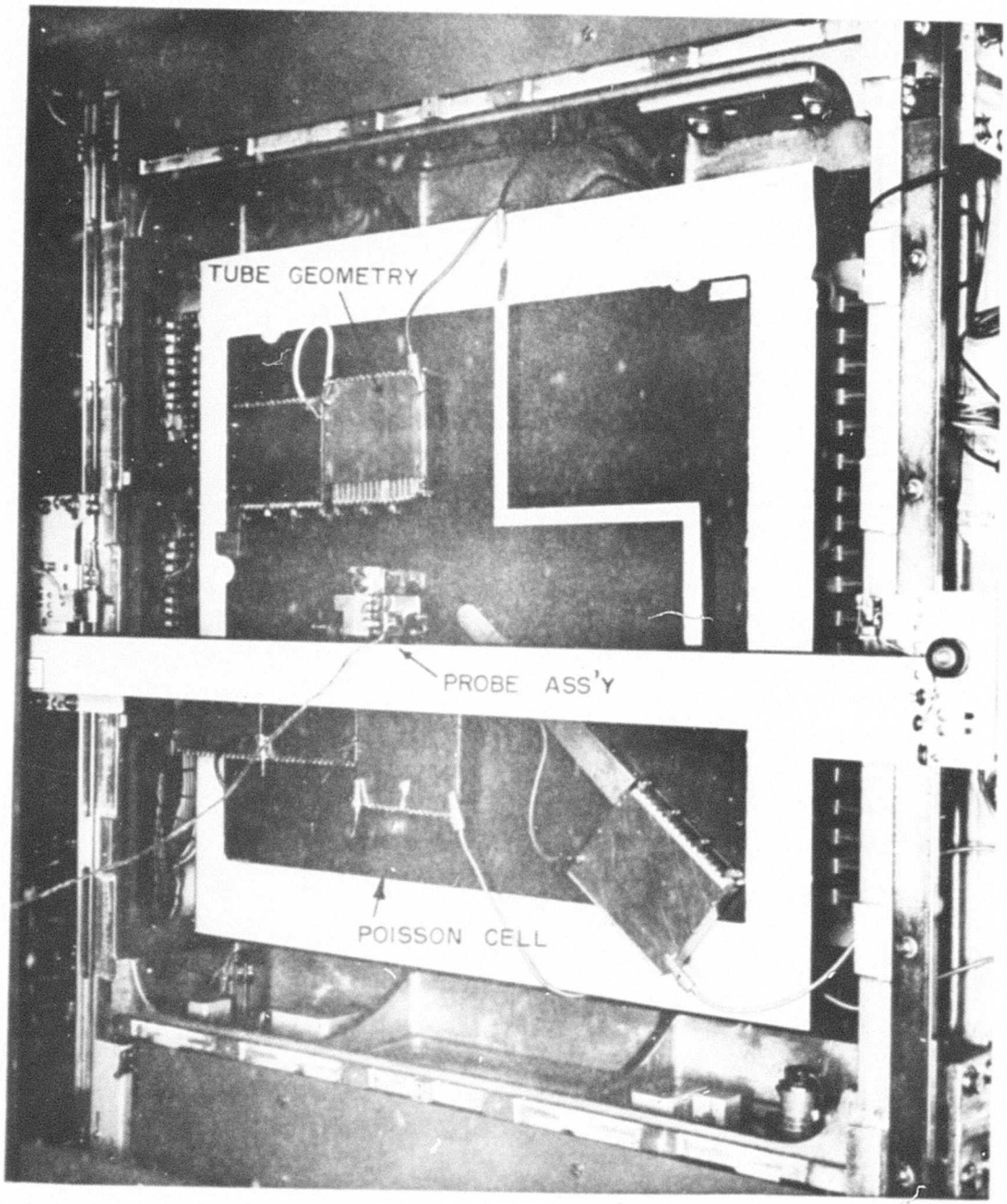

FIG. 6 TOP VIEW OF A MODIFIED X-Y PLOTTER SHOWING THE SIMULATED TUBE GEOMETRY MOUNTED ON POISSON CELL

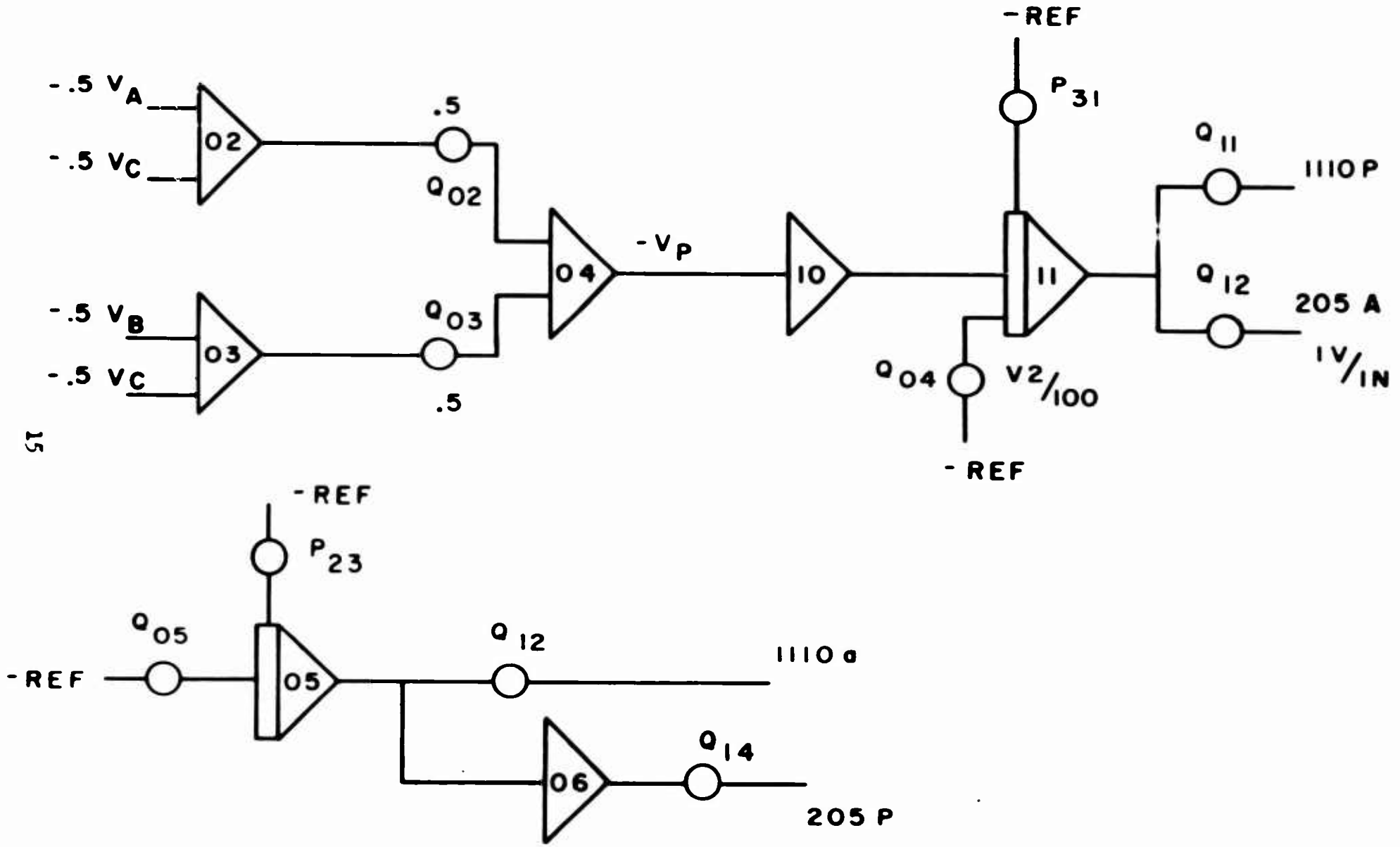

FIG. 7 COMPUTER FLOW DIAGRAM FOR EQUIPOTENTIAL PLOTS

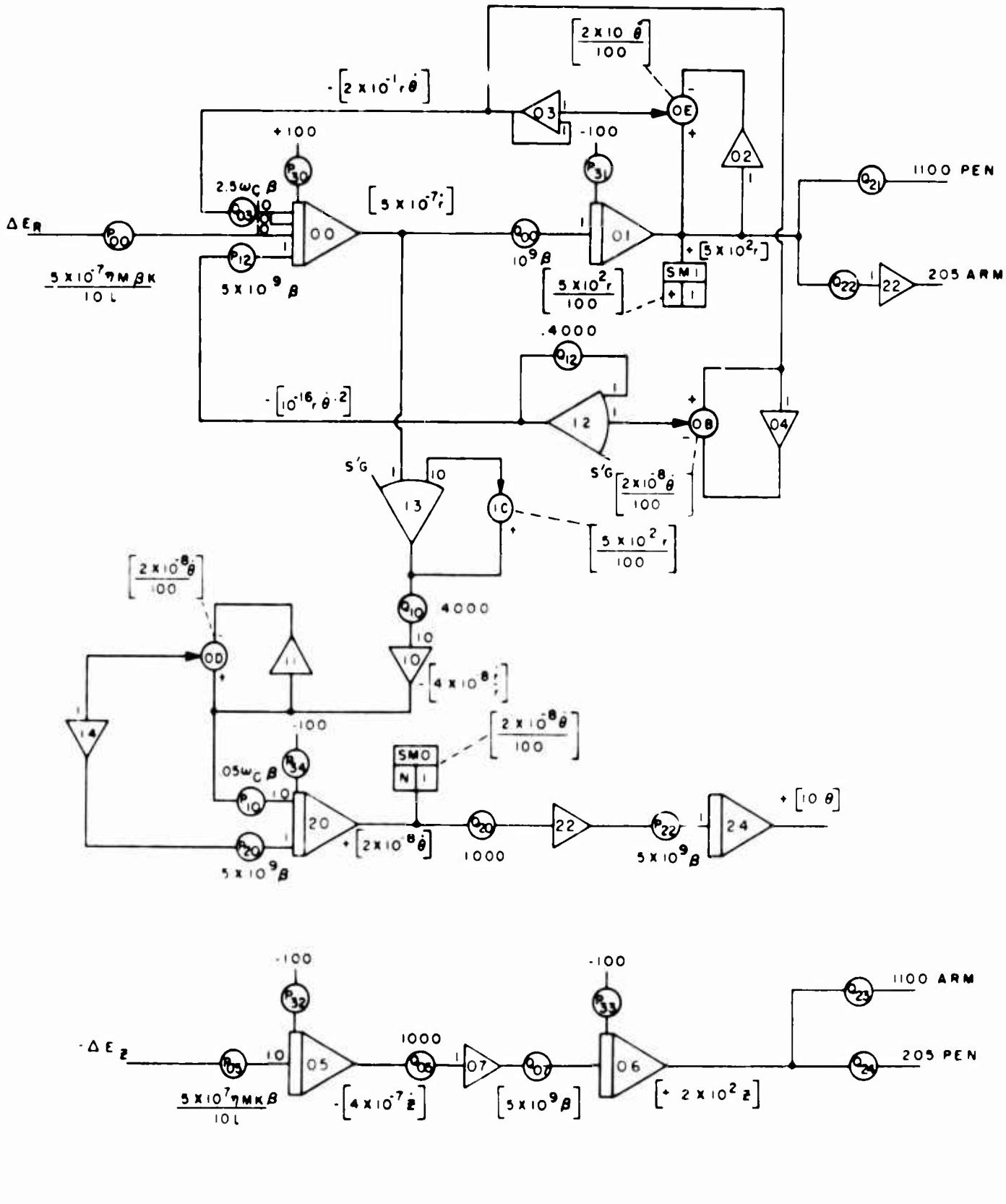

FIG. 8 COMPUTER FLOW DIAGRAM

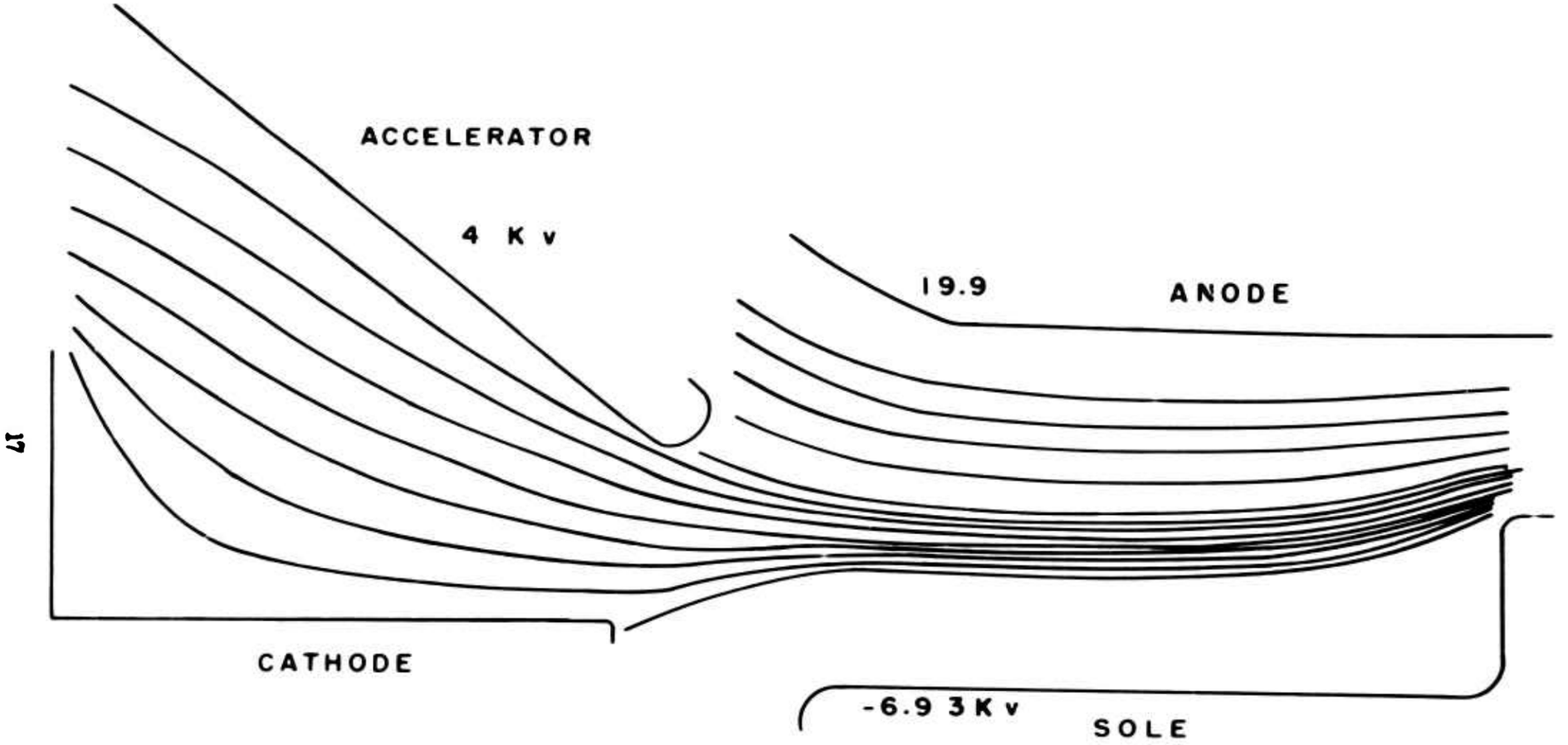

FIG. 9
EQUIPOTENTIAL PLOTS

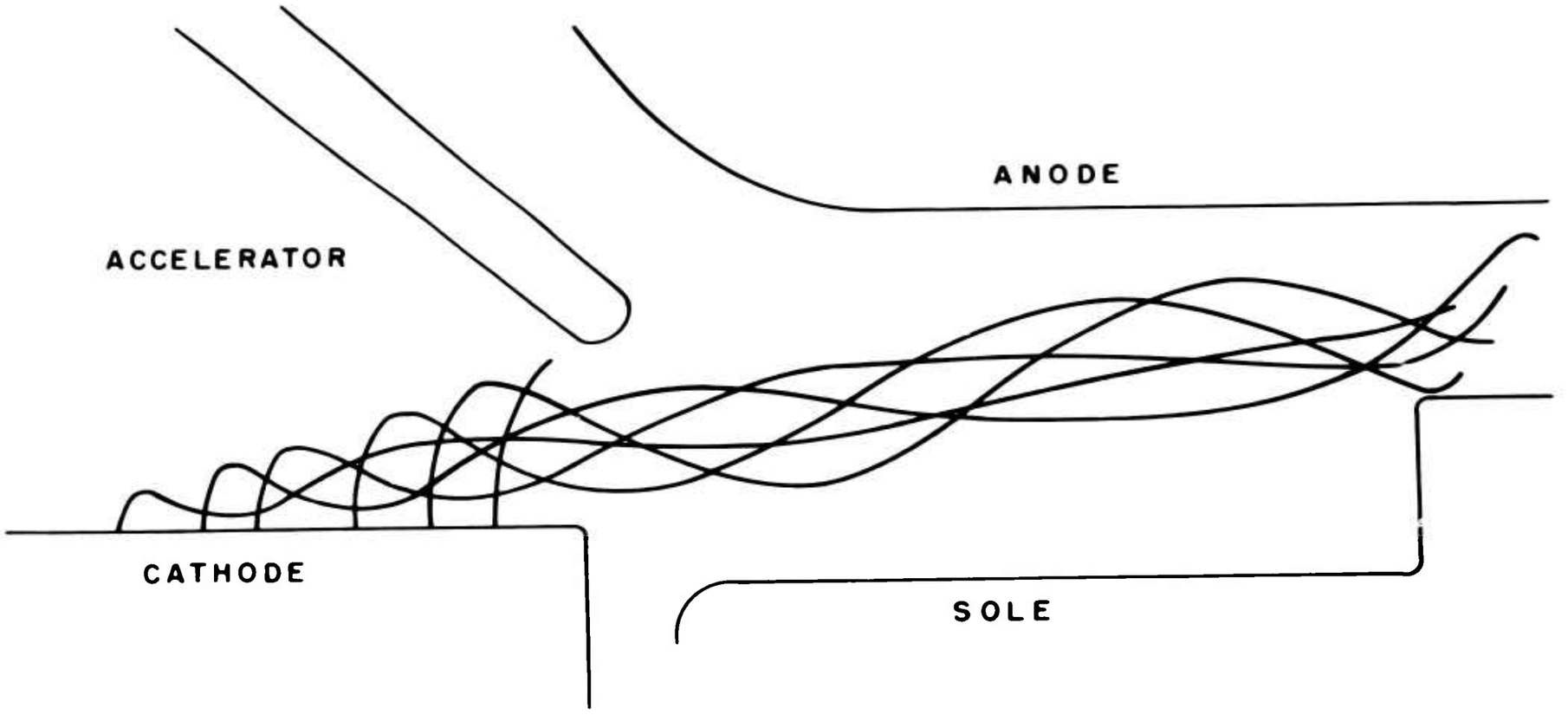

CROSSED-FIELD GUN	
MAGNETIC FIELD	1500 GAUSS
ANODE VOLTAGE	20Kv
ACCELERATOR	10Kv
SOLE	-4Kv
CATHODE TILT	9°

FIG. 10
TRAJECTORY PLOTS

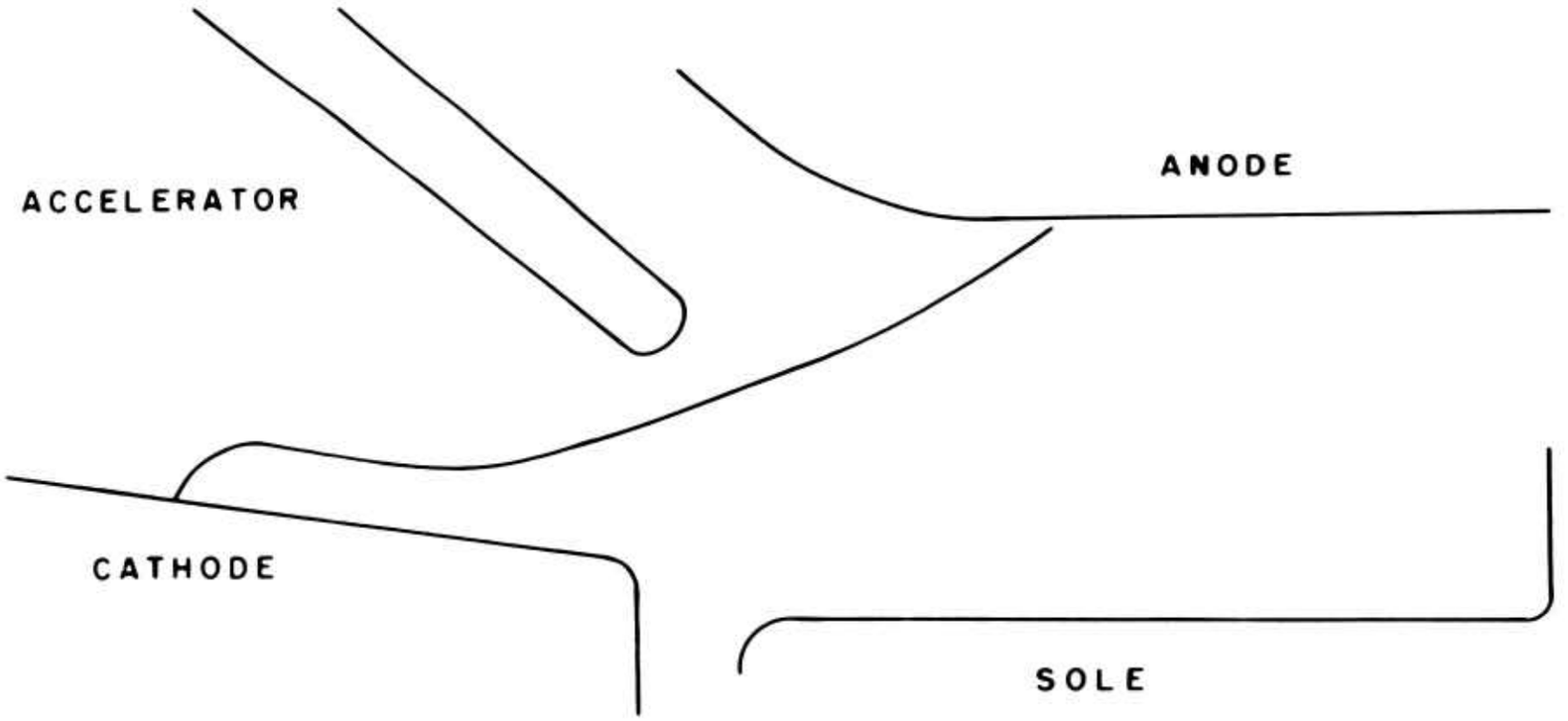

CROSSED-FIELD GUN	
MAGNETIC FIELD	1000 GAUSS
ANODE VOLTAGE	20Kv
ACCELERATOR	4Kv
SOLE	-4Kv
CATHODE TILT	9°

FIG. 11
TRAJECTORY PLOT

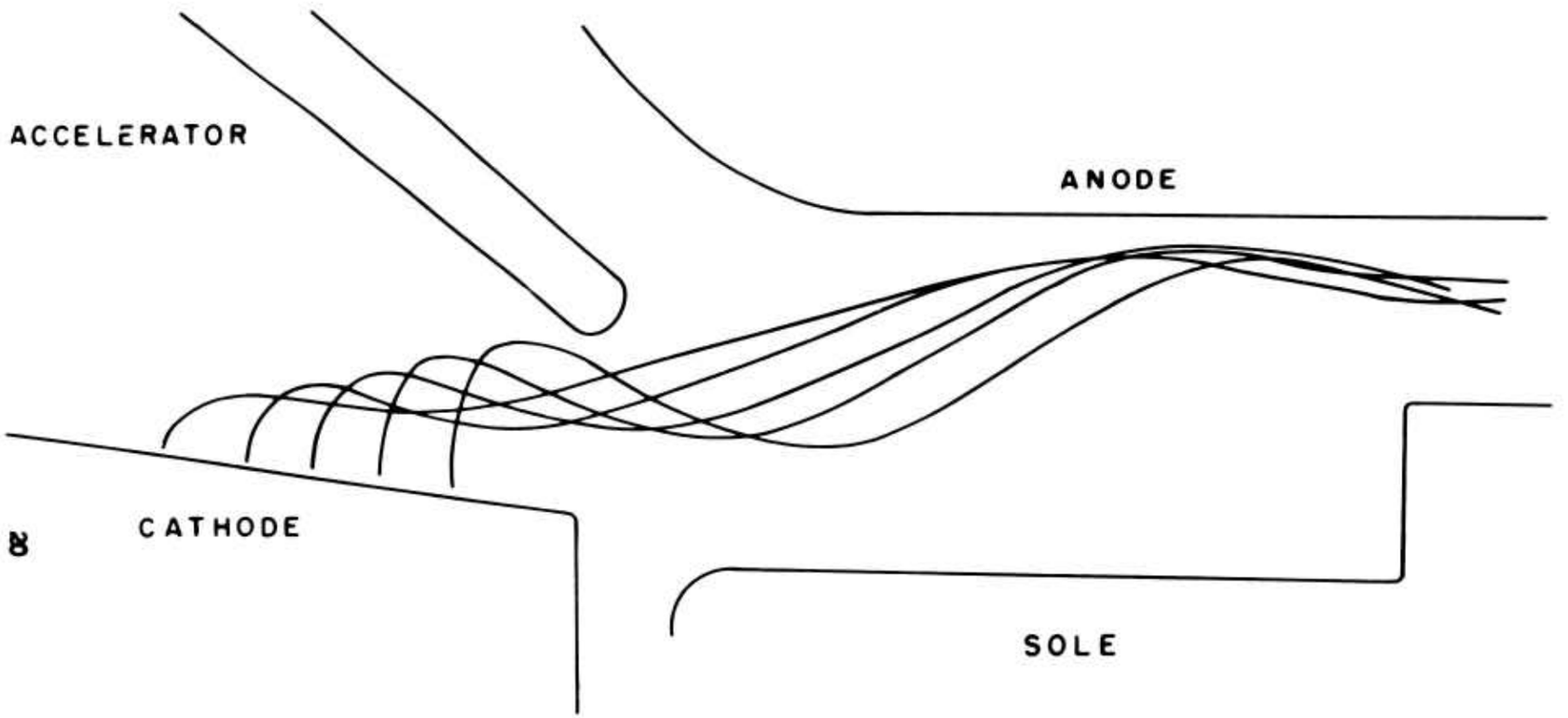

CROSSED-FIELD GUN:

MAGNETIC FIELD	1500 GAUSS
ANODE VOLTAGE	20 K v
ACCELERATOR	10 K v
SOLE	-4 K v
CATHODE TILT	9°

FIG. 12
TRAJECTORY PLOTS

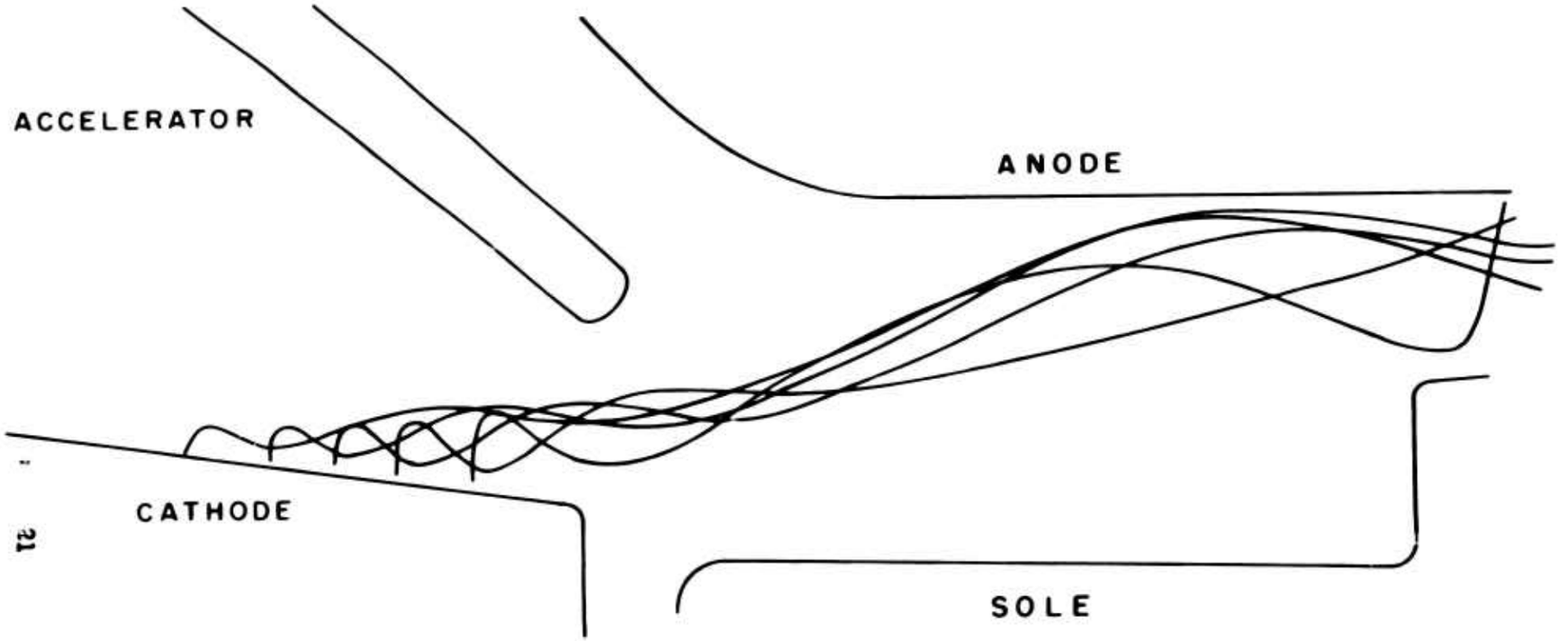

CROSSED-FIELD GUN

MAGNETIC FIELD	1500 GAUSS
ANODE VOLTAGE	20Kv
ACCELERATOR	4Kv
SOLE	-4Kv
CATHODE TILT	9°

FIG.13
TRAJECTORY PLOTS

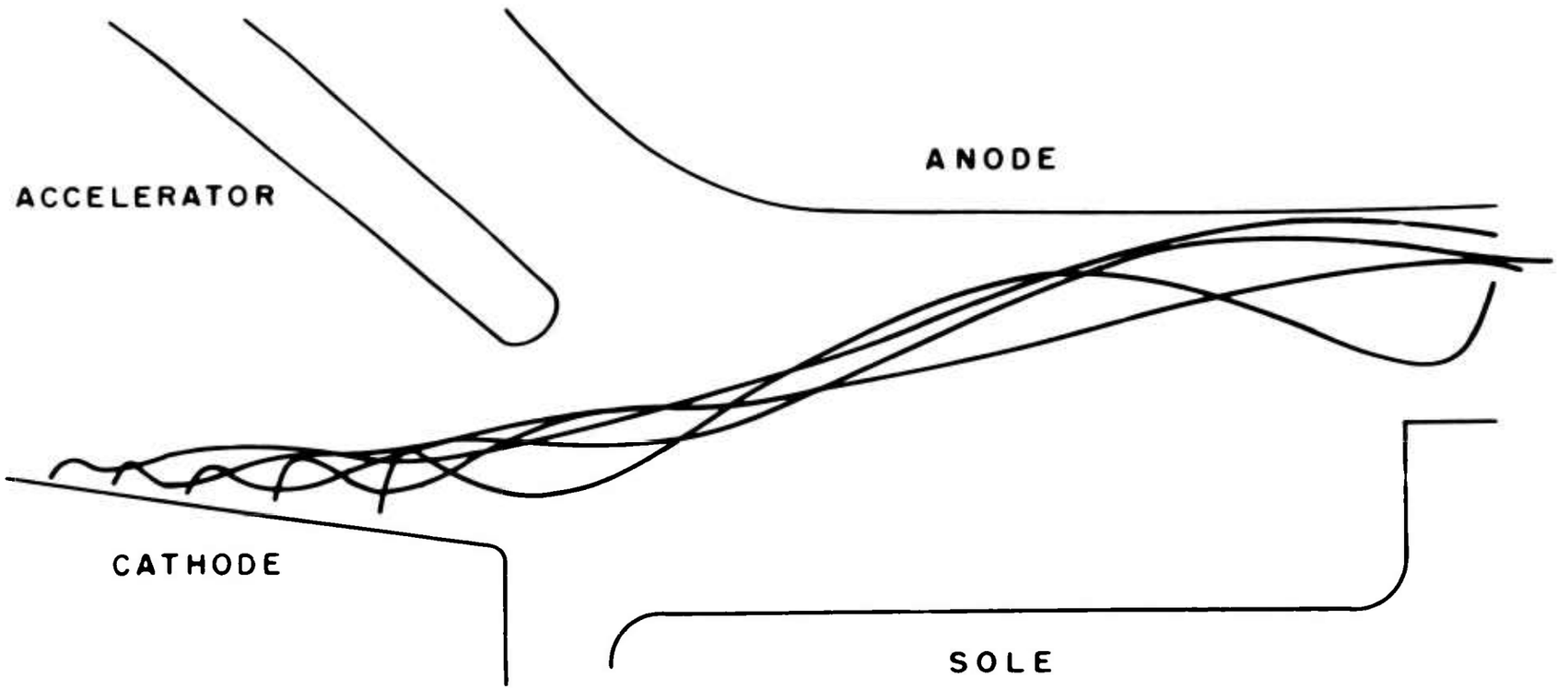

CROSSED-FIELD GUN

MAGNETIC FIELD	1500 GAUSS
ANODE VOLTAGE	20K v
ACCELERATOR	4K v
SOLE	-4K v
CATHODE TILT	9°

FIG. 14
TRAJECTORY PLOTS

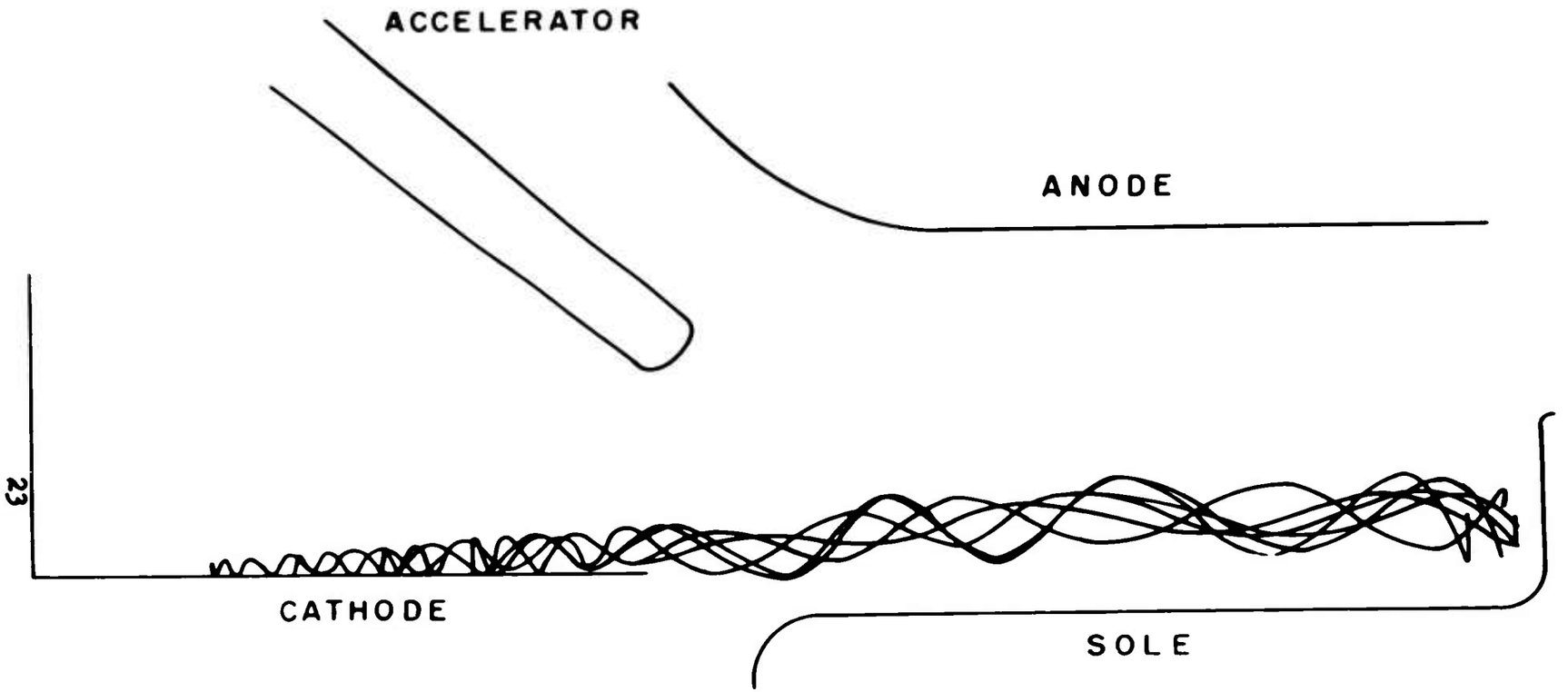

FIG. 15
TRAJECTORY PLOTS

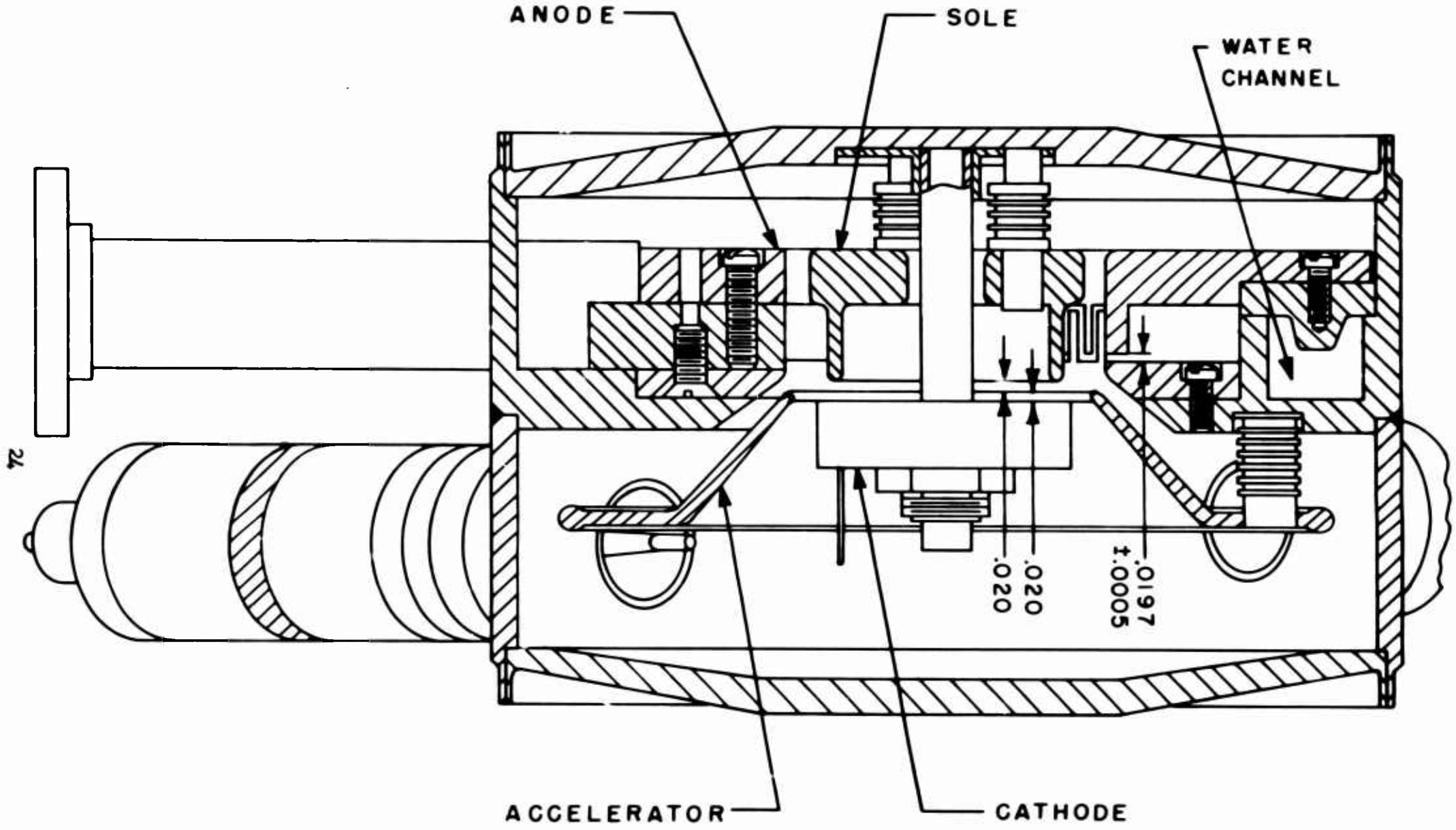

FIG. 16 CROSS SECTION VIEW OF THE GUN AND INTERACTION REGION OF THE M-TYPE BACKWARD-WAVE OSCILLATOR

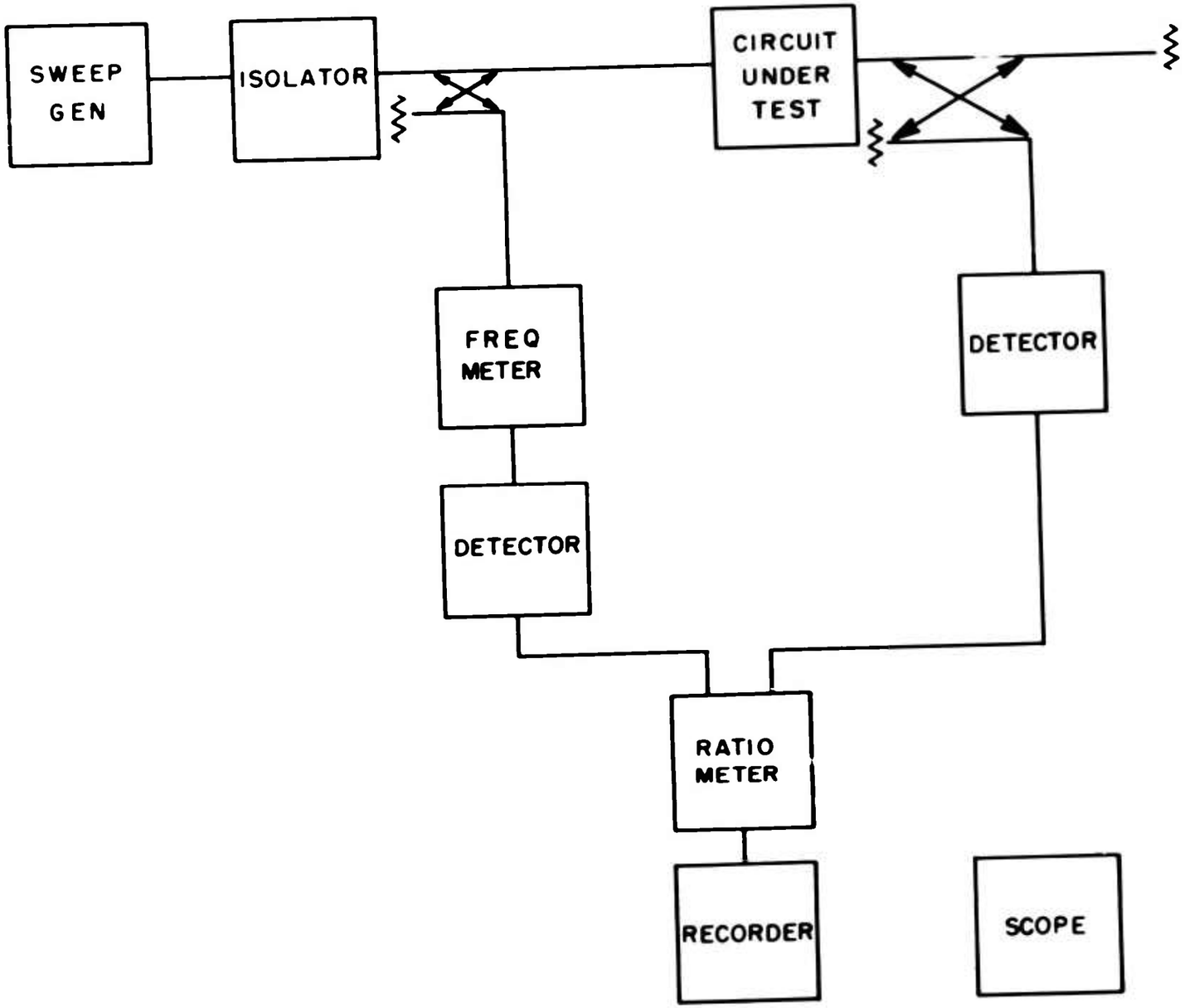

FIG. 17 INSERTION LOSS MEASUREMENTS

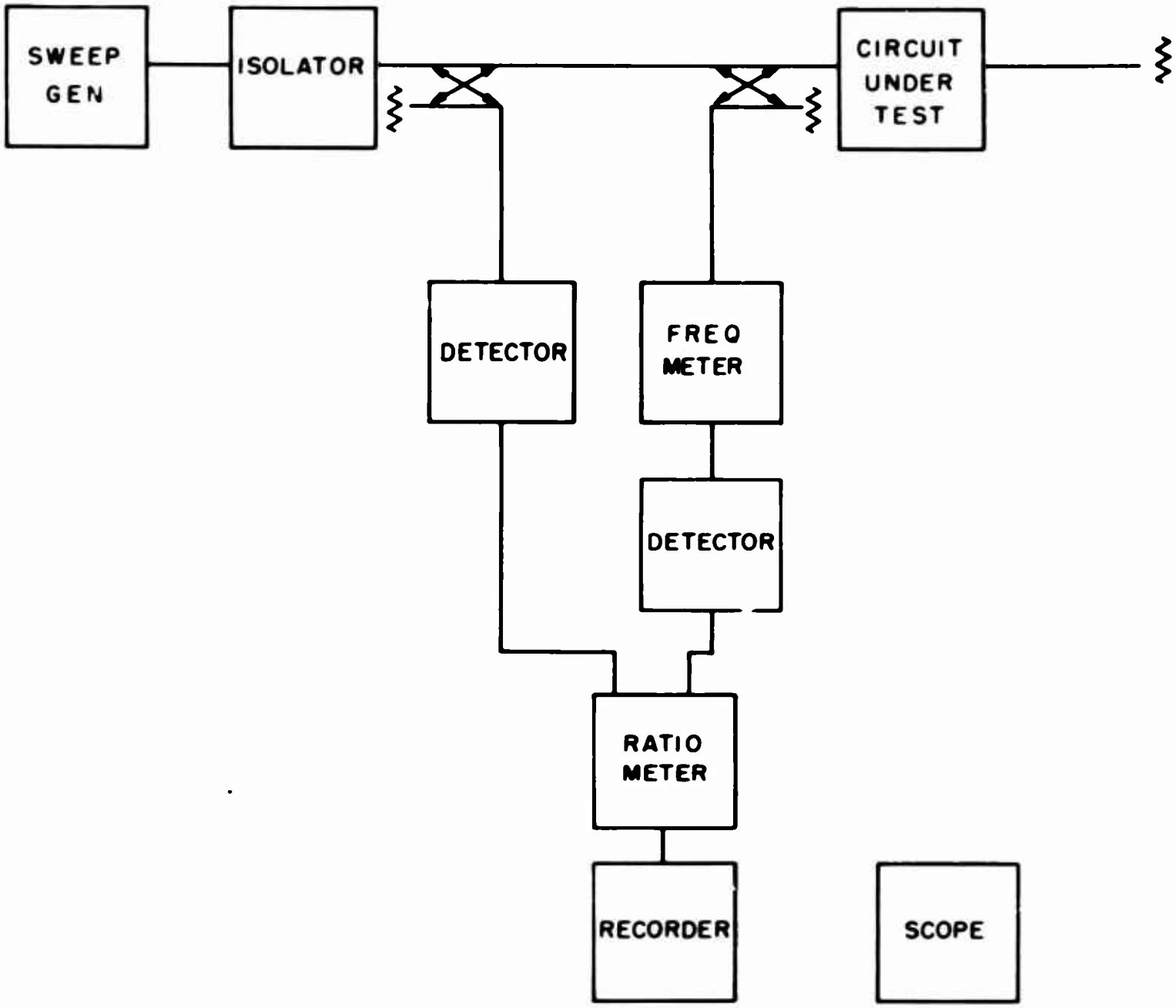

FIG. 18 RETURN LOSS MEASUREMENTS

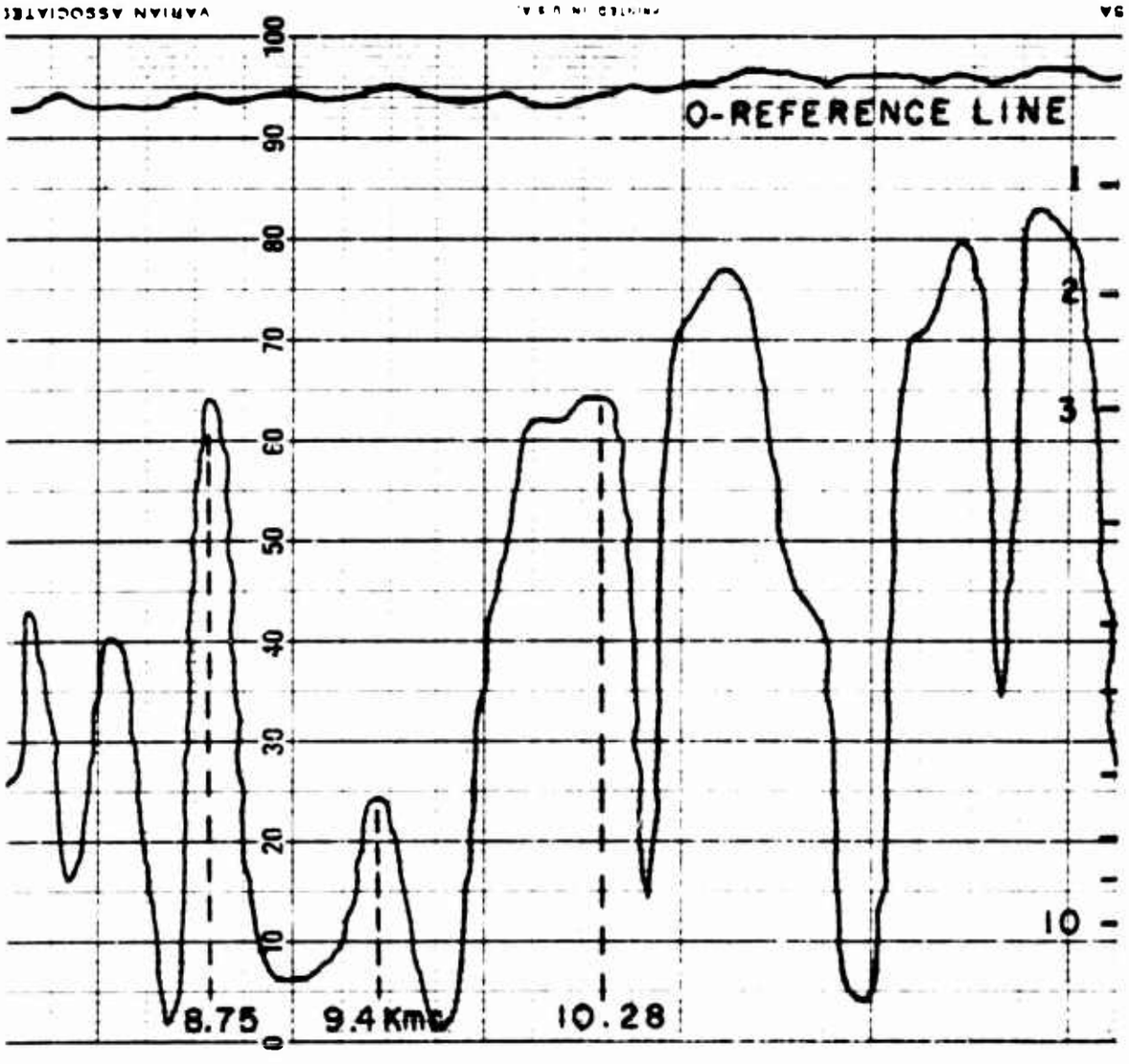

FIG. 19 TUBE RETURN LOSS IN db

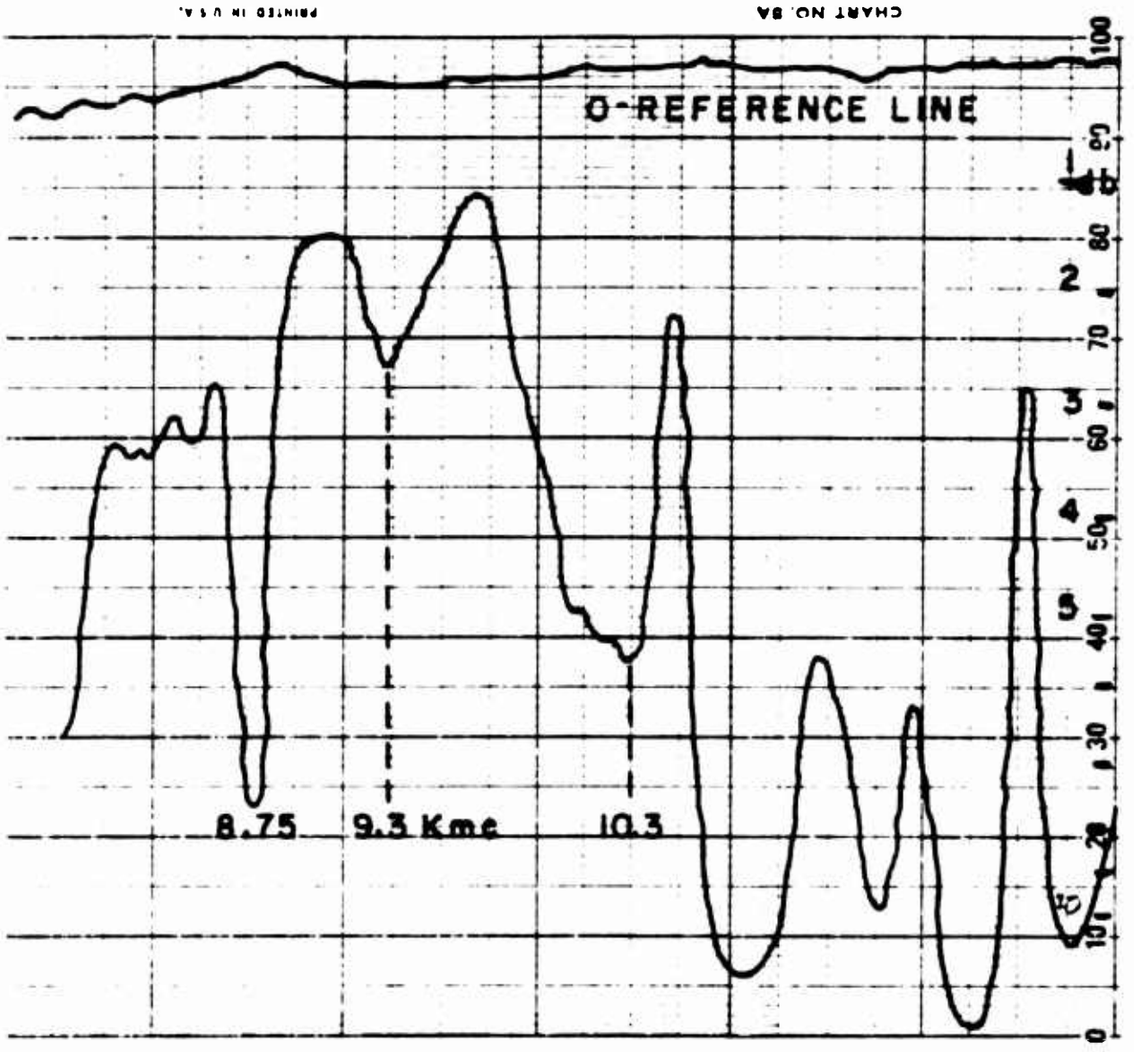

FIG. 20 TUBE INSERTION LOSS IN d b

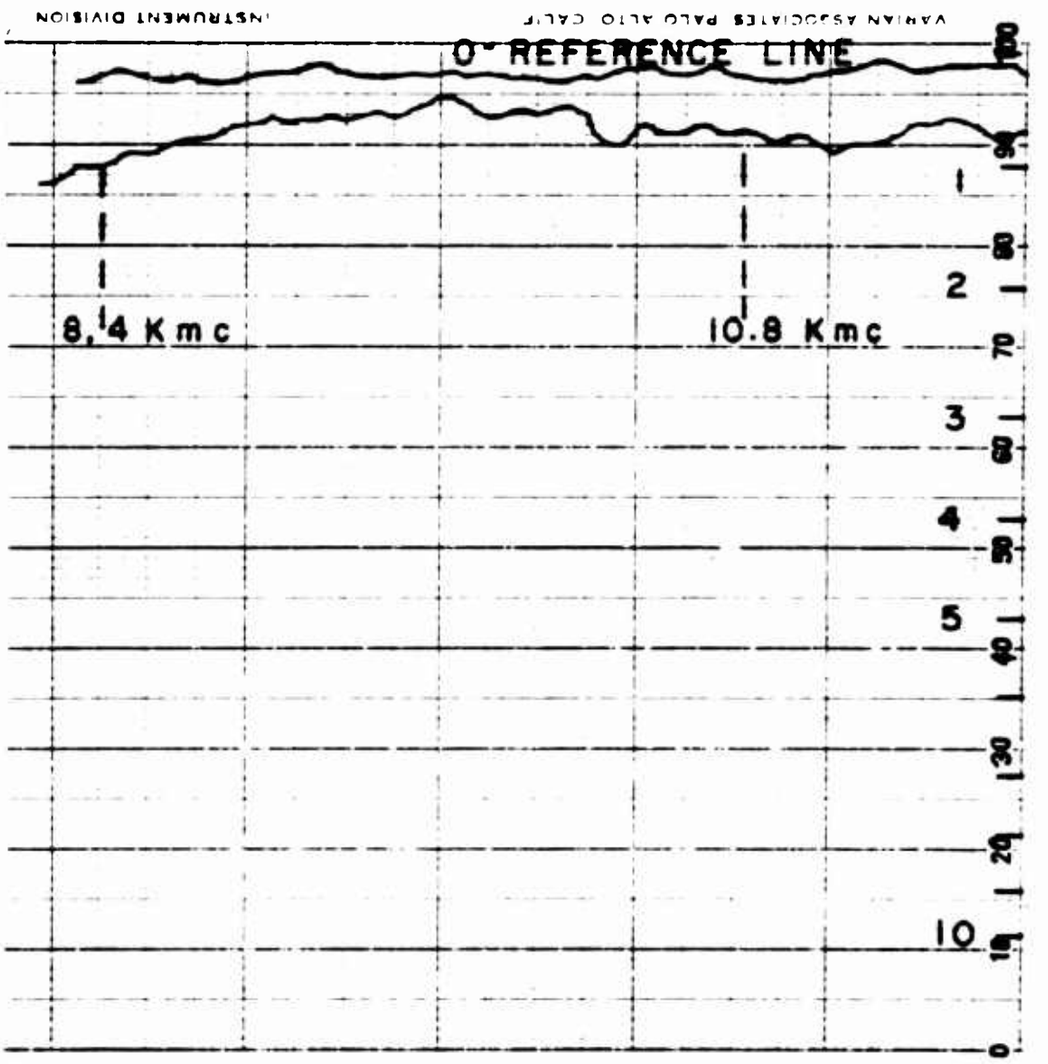

FIG. 21 TUBE WINDOW INSERTION LOSS CHARACTERISTIC IN db

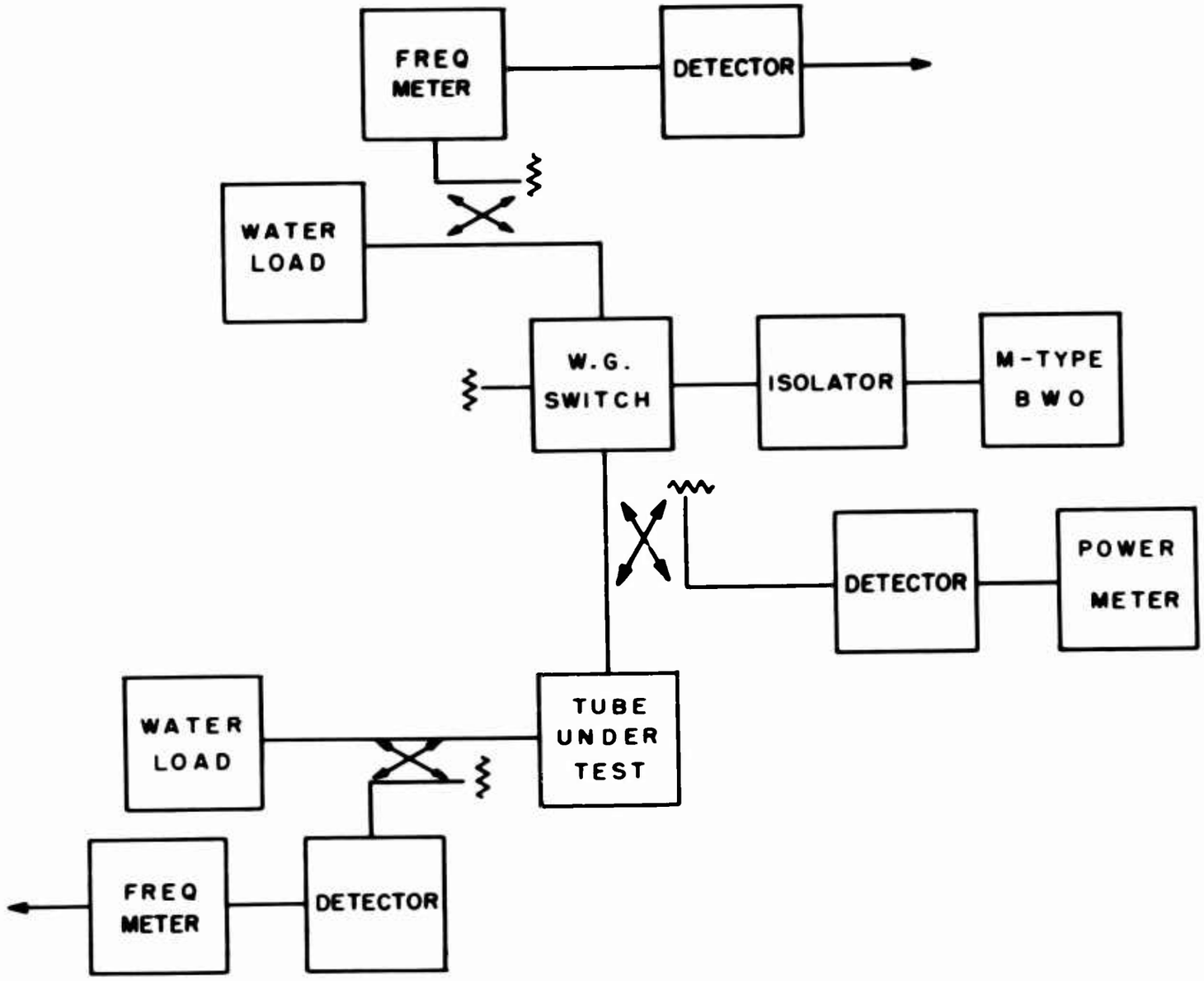

FIG.22 BLOCK DIAGRAM OF TUBE TEST SET-UP

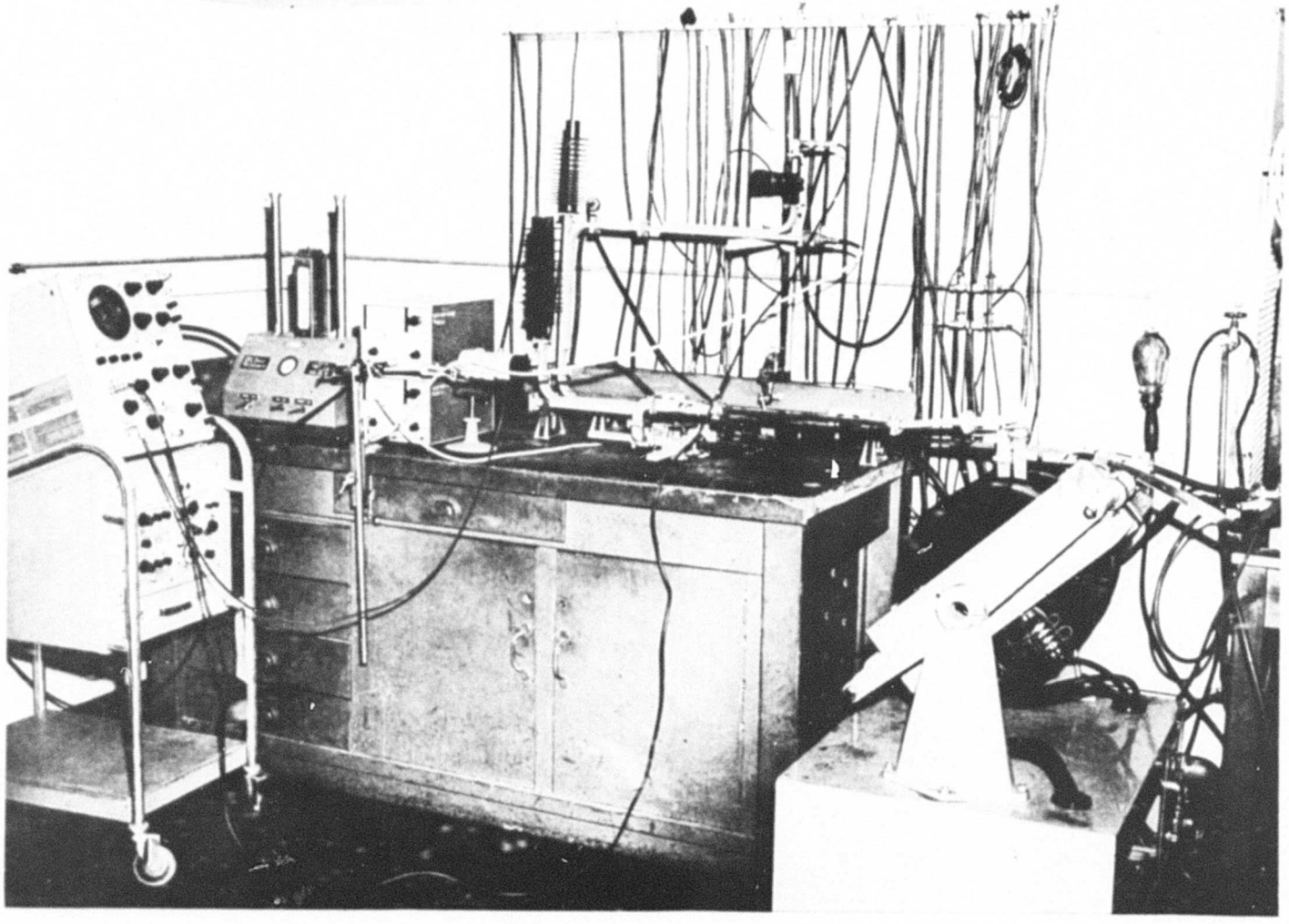

FIG. 23 TEST SET-UP FOR THE X-BAND CROSSED-FIELD TUBE

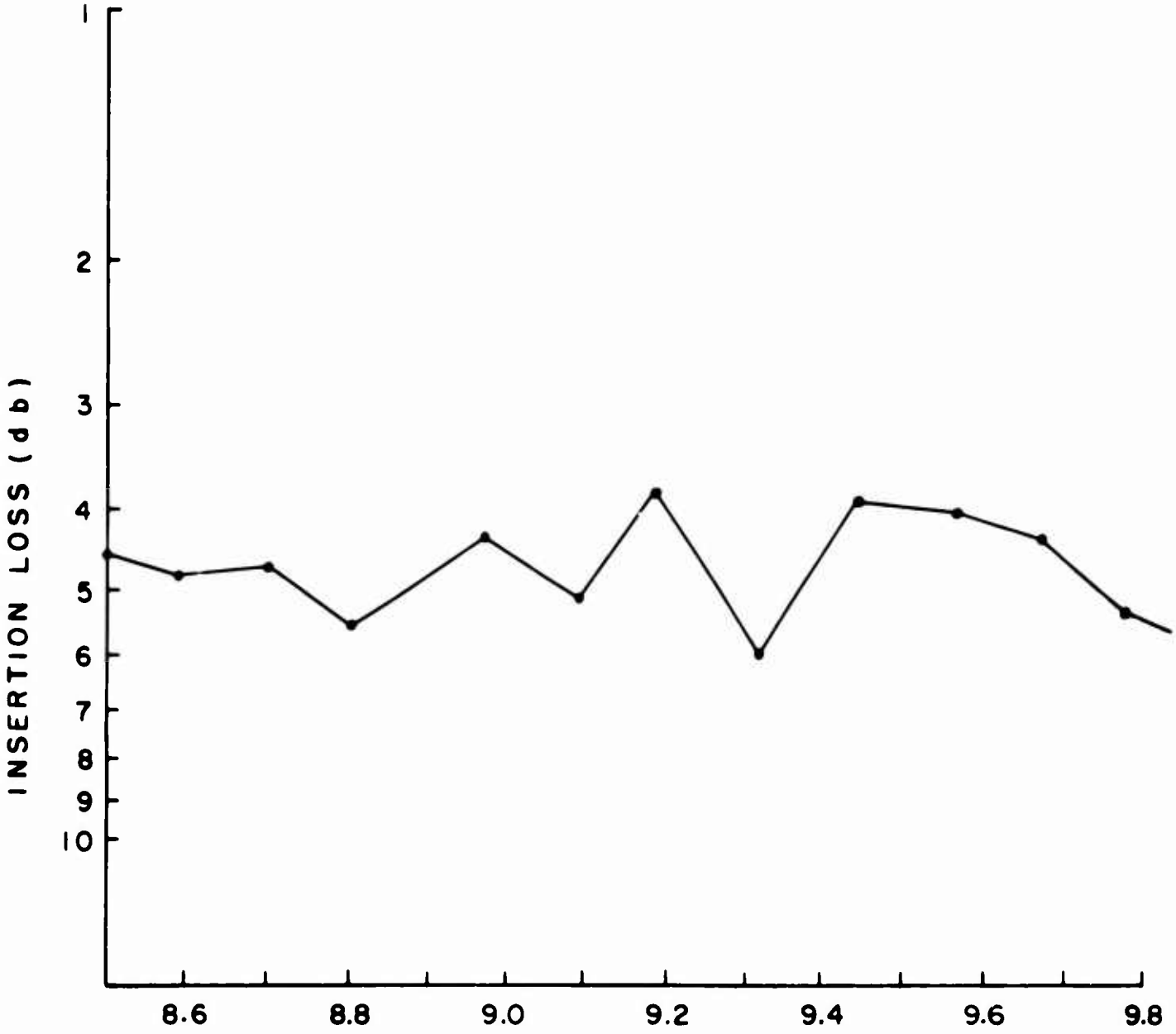

FIG. 24 TUBE INSERTION LOSS

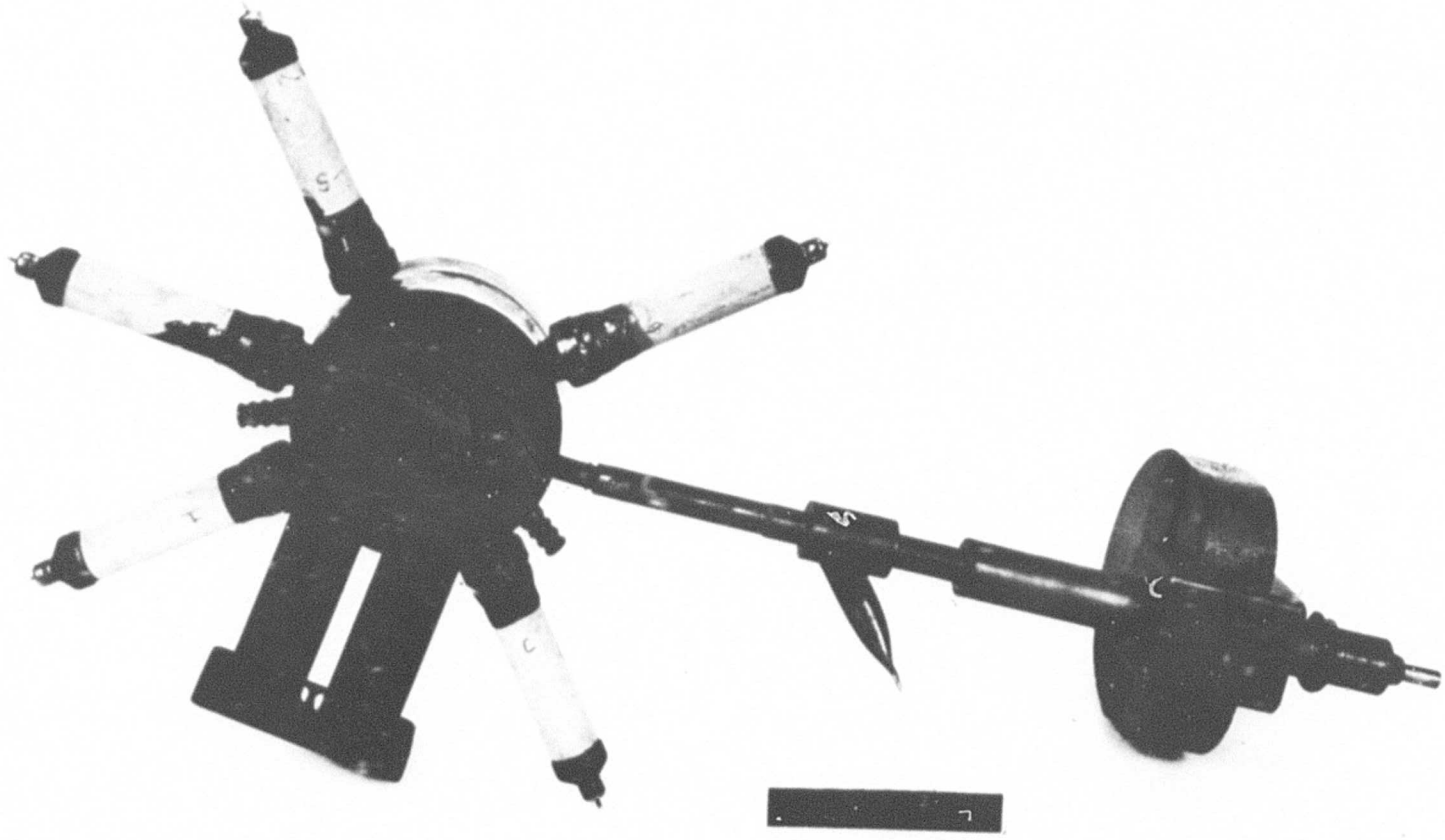

FIG. 25 X-BAND MICROWAVE TUBE (EXPERIMENTAL)

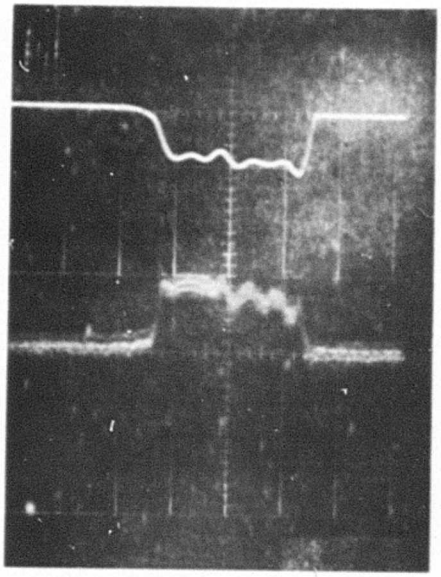

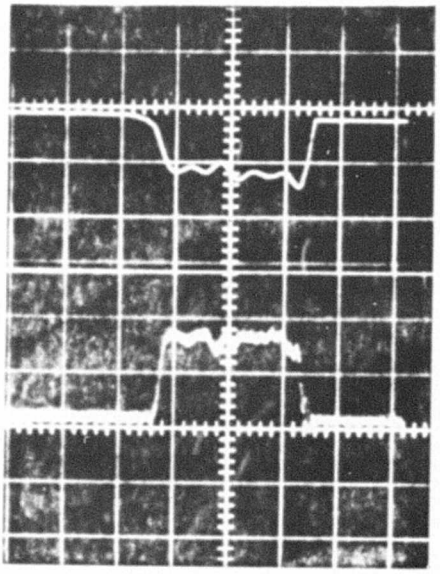

THE UPPER PULSES OF BOTH PICTURES ARE THE VOLTAGE PULSES APPLIED TO THE ACCELERATOR OF THE TUBE. THE OTHER PULSES ARE PICTURES OF THE DETECTED R.F. OUTPUT OF THE TUBE. THE OPERATING CONDITIONS ARE AS FOLLOWS.

	PICTURE #1	PICTURE #2
VOLTAGE PULSE	2.85 Kv	3.42 Kv
ACCELERATOR BIAS VOLTAGE	1.35 Kv	1.3 Kv
SOLE TO CATHODE VOLTAGE	2 Kv	2 Kv
THE BODY TO CATHODE VOLTAGE PULSE	5 Kv	5 Kv
MAGNETIC FIELD	2.6K GAUSS	2.6K GAUSS

FIG. 26 - OSCILLOSCOPE PATTERNS